Accepted Manuscript

Title: DEALING WITH THE UBIQUITY OF PHTHALATES IN THE LABORATORY WHEN DETERMINING PLASTICIZERS BY GAS CHROMATOGRAPHY/MASS SPECTROMETRY AND PARAFAC

Author: M.L. Oca L. Rubio L.A. Sarabia M.C. Ortiz

Please cite this article as: M.L.Oca, L.Rubio, L.A.Sarabia, M.C.Ortiz, DEALING WITH THE UBIQUITY OF PHTHALATES IN THE LABORATORY WHEN DETERMINING PLASTICIZERS BY GAS CHROMATOGRAPHY/MASS SPECTROMETRY AND PARAFAC, Journal of Chromatography A http://dx.doi.org/10.1016/j.chroma.2016.07.074

This is a PDF file of an unedited manuscript that has been accepted for publication. As a service to our customers we are providing this early version of the manuscript. The manuscript will undergo copyediting, typesetting, and review of the resulting proof before it is published in its final form. Please note that during the production process errors may be discovered which could affect the content, and all legal disclaimers that apply to the journal pertain.

DEALING WITH THE UBIQUITY OF PHTHALATES IN THE LABORATORY WHEN DETERMINING PLASTICIZERS BY GAS CHROMATOGRAPHY/MASS SPECTROMETRY AND PARAFAC

M.L. Oca[a], L. Rubio[a], L.A. Sarabia[b], M.C. Ortiz[a,1]

[a]*Department of Chemistry,* [b]*Department of Mathematics and Computation*

Faculty of Sciences, University of Burgos

Plaza Misael Bañuelos s/n, 09001 Burgos (Spain)

[1]Corresponding author. Telephone number: 34-947-259571. *E-mail address*: mcortiz@ubu.es (M.C. Ortiz).

Highlights

- The level of ubiquitous DiBP in solvent blanks was assessed using α and β errors
- PARAFAC succeeds in handling complex finger-peak signals caused by arrays of isomers
- The determination of DiNP based on PARAFAC loadings instead of areas is more reliable
- BHT was proved to be present significantly in a dummy intended for infants

Abstract

Determining plasticizers and other additives migrated from plastic materials becomes a hard task when these substances are already present in the laboratory environment. This work dealt with this drawback in the multiresidue determination of four plasticizers (2,6-di-tert-butyl-4-methyl-phenol (BHT), diisobutyl phthalate (DiBP), bis(2-ethylhexyl) adipate (DEHA) and diisononyl phthalate (DiNP)) and a UV stabilizer (benzophenone (BP)) by gas chromatography/mass spectrometry (GC/MS) using DiBP-d_4 as internal standard. The ubiquity of DiBP by a non-constant leaching process in the laboratory was detected, which could not guarantee the achievement of a trustworthy quantification. To handle this, the assessment of the level of DiBP in solvent blanks having fixed the probabilities of false non-compliance (α) and false compliance (β) at 0.01 was performed. On the other hand, another special case was that of DiNP, in whose chromatogram finger peaks appear because of an array of possible C_9 isomers. PARAFAC, used for the identification and quantification of all the substances, is a useful chemometric tool that enabled a more reliable determination of this analyte since no peak areas were considered but chromatographic and spectral loadings.

Since phthalates may migrate from rubber latex items, an evaluation of the existence of matrix effects on the determination of the five analytes was conducted prior to an extraction with hexane from a dummy for infants. As matrix effects were present, the quantification of the compounds under study was performed following the standard addition method using PARAFAC sample loadings as response variable. As a result, the presence of BHT was confirmed, being its concentration equal to 37.87 µg L^{-1}. Calibrations based on PARAFAC yielded the following values for the decision limit (CCα): 1.16 µg L^{-1} for BHT, 1.34 µg L^{-1} for BP, 1.84 µg L^{-1} for DEHA and 51.42 µg L^{-1} for DINP (for $\alpha = 0.05$ and two replicates).

1. Introduction

Alkyl and aryl esters of 1,2-benzenedicarboxylic acid, better known as phthalates, are a group of synthetic compounds widely used as plasticizers. Mainly added to polyvinyl chloride

(PVC), phthalates increase plastic flexibility, resistance and durability. Widely used items such as toys, water pipes, wallpaper, artificial leather, electrical wire insulation, glue, cosmetics, plastic water bottles, paints and printing ink include phthalate additives in their formulation, and as a result, a huge worldwide market has been created around these compounds. However, phthalates have been classified as endocrine disrupting chemicals and potential human carcinogenic agents [1,2,3,4]. They can be easily leached out from plastic materials over time since they are not chemically bound to the polymeric matrix. Due to a direct migration process from packaging films and plastic containers, phthalates can thus be found in a high concentration in foodstuffs and beverages, especially in fatty products because of the hydrophobia of these chemicals [5,6,7,8]. They can even be released into the air [9,10]. In this context, the EU Regulation No 10/2011 [11] only permits a limited use of certain phthalates in food contact materials by establishing specific migration limits (SMLs) on the basis of toxicological evaluations by the European Food Safety Authority.

Aside from health concerns, their ubiquity can cause frustration and big trouble when analysing them, especially if trace analyses of phthalates by chromatographic methods are to be carried out [12,13]. Cross-contamination during the analytical procedure often leads to false positive or overestimated results, while actually only a part of the predicted concentration should have been related to the sample. Phthalates are indeed everywhere in the laboratory environment, including solvents, chemicals, glassware, gloves and consumables, such as rubber tubing, syringes, pipette tips, filters, stir bars, vials, 96-we ll plates, caps, etc. [12,13]; even both the chromatographic system and laboratory air may be sources of contamination [12]. So a great probability of phthalate interferences exists whenever gas-chromatography and/or liquid-chromatography analyses are performed. Common phthalate-origin lab interferents are diisobutyl phthalate (DiBP), di(2-ethylhexyl)

phthalate, di-n-butyl phthalate, diisononyl phthalate (DiNP), butyl benzyl phthalate, di-n-octyl phthalate and dimethyl phthalate [14]. Among them, the first three compounds are mainly involved in lab environment and blank issues, especially the latter two due to their low molecular weight, easy partition from polymer matrix, solubility in water and high usage in PVC production [13].

Several strategies to reduce the presence of phthalate contaminants have been developed [12,15,16], such as avoiding plastic labware, baking out glassware or rinsing it with redistilled solvents. However, even so, this problem is proving to be very difficult to get rid of, so usually there is no choice but to take its existence into account and face it. Nevertheless, some guarantees should be first established in order to be able to distinguish significantly the amount of phthalates present in a blank from that in a sample. This would be easy to achieve if the blank concentration profile of the contaminant displayed a constant pattern, so that the blank average value could be subtracted to determine the amount of the phthalate under study in the sample. But if this is not the case and a variable leaching behaviour is detected, difficulties arise, because now the blank average value would not be representative of the true presence of the interferent in the laboratory environment. This drawback could be

tackled by using the approach proposed in this work, which has consisted in i) estimating the probability distributions of the concentration in blanks and standards at a fixed level of the controversial contaminants, and then ii) after setting the probability of making a type I error (α) and that of a type II error (β), computing the critical or rejection concentration value beyond which the amount of interferents in a sample is statistically higher than that at the blank level. A more detailed explanation on the use of this methodology in analytical measurements can be found in [17,18].

The determination of DiBP and DiNP by gas-chromatography coupled to mass spectrometry (GC/MS) has been pursued in this work, being the former variably ubiquitous while performing the study. No restrictive regulations are established on DiBP regarding its use in plastic manufacturing, so the generic SML of 60 mg kg^{-1} should apply according to [11]. On the other hand, DiNP (in the form of diesters of the phthalic acid, with primary saturated C_8-C_{10} branched alcohols, being C_9 more than 60%) is only authorised to be used as additive or polymer production aid within the European Union, and a total SML of 9 mg kg^{-1} is set [11]. In this work, these SML values have been taken into account for the performance of the procedure. Due to the composition of the chemical marketed as DiNP, its signal typically appears in the chromatogram as finger peaks instead of a single one because of an array of C_9 isomers (with alkyl groups with different degree of branching on both side chains of the phthalic ring) that were impossible to separate before commercializing. In fact, there are two main CAS numbers available for DiNP from several manufacturers: DiNP 1 (CAS no. 68515-48-0), which is a mixture of isomers with alkyl chains from 8 to 10 (mainly 9) carbons long, and DiNP 2 (CAS no. 28553-12-0), composed exclusively of C_9-chains [19,20]. Anyway, a quantitation based on the area summation integration of that signal could lead to unreliable results, either greater or lower than the true ones, because of the complex shape of those peaks. However, the statistical methodology Parallel Factor Analysis (PARAFAC) decomposition, used in this work not only to quantify the analytes, but also to identify them unequivocally by taking advantage of the second-order property of the GC/MS data, offers a more trustworthy approach to deal with complex signals such as that of DiNP. Ensuring the unequivocal presence of every analyte in a sample is a key question when target analyses are performed, as official regulations and guidelines [21,22,23] lay down in the form of tolerance interval requirements. This identification, based on the unique mass spectrum and elution time profiles estimated by PARAFAC, guarantees the specificity of the analysis, even though shared ions are present at the same retention time.

As well as these two phthalate derivatives, the multiresidue gas-chromatography method developed in this work also pursues the determination of benzophenone (BP), 2,6-di-tert-butyl-4-methyl-phenol (BHT) and bis(2-ethylhexyl) adipate (DEHA). BP is widely used as a flavour ingredient, a fragrance enhancer, in the manufacture of insecticides, agricultural chemicals, hypnotic drugs, antihistamines and other pharmaceuticals; but its main application comes from its ultraviolet (UV)-curing property, which makes it suitable for being added to plastic packaging as a UV blocker. This allows manufacturers to package their products in clear glass or plastic rather than opaque or dark packaging to prevent them from being damaged [24]. DEHA is a common plasticizer primarily used together with phthalates in the PVC industry, while BHT is a manufactured antioxidant commonly used as preservative in plastics, rubber, petroleum products, foods, pharmaceuticals and cosmetics. These three substances are allowed to be used as additive or polymer production aid within

the European Union, being the values of their SMLs equal to 0.6 mg kg^{-1} for BP, 3 mg kg^{-1} for BHT and 18 mg kg^{-1} for DEHA [**11**]. Diisobutyl phthalate-3,4,5,6- d$_4$ (DiBP-d$_4$) has been used as the chromatographic internal standard (IS) for the five analytes of interest.

The presence of these five compounds in the natural rubber latex forming a dummy intended for infants has also been studied, and their leaching into a volume of hexane has thus been tested. But firstly, in order to ensure a proper determination of every substance in these samples, the existence of matrix effects has been evaluated and confirmed. This fact has led to the decision of estimating the concentration of each analyte leached into the volume of hexane by means of the standard addition methodology.

2. Material and methods

2.1. Chemicals

Benzophenone (CAS no. 119-61-9; purified by sublimation), 2,6-di-tert-butyl-4-methyl-phenol (CAS no. 128-37-0), diisobutyl phthalate (CAS no. 84-69-5), diisobutyl phthalate-3,4,5,6-d$_4$ (CAS no. 358730-88-8; analytical standard), bis(2-ethylhexyl) adipate (CAS no. 103-23-1) and diisononyl phthalate (CAS no. 28553-12-0; ester content ≥ 99%, mixture of C$_9$ isomers), all of 99% or higher purity, were purchased from Sigma-Aldrich (Steinheim, Germany). n-Hexane (CAS no. 110-54-3; for liquid chromatography Lichrosolv®) was obtained from Merck KGaA (Darmstadt, Germany).

2.2. Standard solutions

Stock solutions were prepared individually in hexane at a concentration of 1000 mg L^{-1} for BHT and BP, of 700 mg L^{-1} for DiBP-d$_4$ and of 2000 mg L^{-1} for DiBP, DEHA and DiNP. Intermediate solutions were prepared from the previous ones by dilution in the same solvent. All the solutions were kept in crimp vials, stored at low temperature (4ºC) and protected from light. Table 1 shows the standards and/or samples analysed (concentration ranges and number of standards) together with the dimensions of the data tensors for each experimental stage of this work (Sections 4.1 to 4.4). Regarding the step related to the procedure to assess the level of DiBP, as can be seen in Table 1, the solvent blanks and standards were analysed in two days due to the impossibility of carrying out the whole analysis within the same day. The data from the analysis of 2 out of the 24 solvent blanks containing IS and the 22 non-zero solvent standards performed the first day were also used to estimate the calibration models for BHT, BP, DEHA and DiNP (see Section 4.1.2).

Only glassware was used throughout all this study, and plastic consumables were avoided as far as possible. A thorough procedure for cleaning the lab glassware was followed to try to minimize cross-contamination from plasticizers.

2.3. Extraction in hexane conditions

The surface of a dummy for infants was placed in a beaker with 60 mL of hexane for 1 hour to perform an exhaustive extraction of the potential migrants. The beaker was covered with a watch glass in order to minimize the evaporation of the solvent. This extraction experiment was performed at room temperature. After 1 hour, the dummy was removed and fresh hexane was added till reaching up the original volume again. This extract was stored under refrigeration at 4⁰C and used to perform the standard addition method.

2.4. GC/MS analysis

Analyses were carried out on an Agilent 7890A gas chromatograph coupled to an Agilent 5975C mass spectrometer detector (Agilent Technologies, Santa Clara, CA, USA). The analytical column used was an Agilent HP-5MS Ultra Inert (30 m × 0.25 mm i.d., 0.25 μm film thickness). Helium was used as the carrier gas at a constant flow of 1.3 mL min^{-1}, and the initial pressure was set at 10.121 psi.

Injections were performed using the MultiPurpose Sampler MPS2XL from GERSTEL GmbH & Co. KG (Mülheim an der Ruhr, Germany) with a 10 μL syringe. The injection system consisted of a PTV inlet with a septumless head (CIS 6 from GERSTEL) equipped with a straight-with-notch quartz glass liner. A volume of 1 μL was injected at a controlled speed of 1 μL s^{-1}. Before and after each injection, the syringe was washed twice with acetone and twice with hexane, while ten washings with acetone and hexane were carried out after each injection throughout the measurement of the standard addition samples. The injection penetration was set at 40 mm, whereas the vial penetration was 30 mm. Amber glass vials were used for the analyses. The PTV inlet operated in the cold splitless mode. During the injection and for 0.1 min afterwards, the inlet temperature was 55⁰C; this temperature was ramped then at 12⁰C s^{-1} from that initial value up to 270⁰C, which was held for 15 min. The septum purge flow rate was set at 3 mL min^{-1} while the purge flow rate through the split vent was 30 mL min^{-1} from 0.6 min to 2 min. After 2 min, the flow rate was set at 20 mL min^{-1}.

The oven temperature was maintained at 40⁰C for 0.6 min. Then the temperature was increased at 20⁰C min^{-1} to 250⁰C, which was maintained for 1 min and next programmed at 10⁰C min^{-1} to 290⁰C, which was held for 3 min. The run time was 19.1 min. A post run step was performed at 300⁰C for 4 min.

After a solvent delay of 8 min, the mass spectrometer was operated in the electron impact (EI) ionization mode at 70 eV. The transfer line temperature was set at 300°C, the ion source temperature at 230°C and the quadrupole temperature at 150°C. Data were acquired in single ion monitoring (SIM) mode. Five acquisition windows for SIM data were used: i) for BHT (start time: 8 min, ion dwell time: 30 ms), the following m/z ratios were selected: 91, 145, 177, 205 and 220; ii) for BP (start time: 8.80 min, ion dwell time: 30 ms), the diagnostic ions were 51, 77, 105, 152 and 182; iii) for DiBP and DiBP-d$_4$ (start time: 9.80 min, ion dwell time: 10 ms), where the diagnostic ions for DiBP were 104, 149, 167, 205 and 223, and the diagnostic ions for DiBP-d$_4$ were 80, 153, 171, 209 and 227; iv) for DEHA (start time: 12 min, ion dwell time: 30 ms), the m/z ratios recorded were 112, 129, 147, 241 and 259; v) for DiNP (start time: 14.60 min, ion dwell time: 25 ms), the diagnostic ions were 57, 127, 149, 167, 275 and 293.

2.5. Software

MSD ChemStation E.02.01.1177 (Agilent Technologies, Inc.) with Data Analysis software was used for data acquisition and processing. The NIST mass spectral library [25] was also used. PARAFAC and PARAFAC2 decompositions were performed with the PLS_Toolbox 6.0.1 [26] for use with MATLAB [27] (The MathWorks, Inc.). The building and validation of all the regression models as well as the comparison of some of them and the fitting of the probability distributions were carried out using STATGRAPHICS Centurion XVI [28]. Decision limit (CCα) and capability of detection (CCβ) were calculated with the DETARCHI program [29].

3. Theory

3.1. PARAFAC and PARAFAC2 decompositions

In the case of three-way data, PARAFAC decomposes a data tensor $\underline{\mathbf{X}}$ into triads or trilinear factors [30] and each factor consists of three loading vectors. GC/MS data can be arranged in a three-way array $\underline{\mathbf{X}}$ (of dimension $I \times J \times K$), where for each of the K samples analysed, the abundance measured at J m/z ratios is recorded at I elution times around the retention time of each compound. In this case, the trilinear PARAFAC model is:

$$x_{ijk} = \sum_{f=1}^{F} a_{if} b_{jf} c_{kf} + e_{ijk}, \quad i = 1, 2, \ldots, I; \quad j = 1, 2, \ldots, J; \quad k = 1, 2, \ldots, K \tag{1}$$

where F is the number of factors, $\mathbf{a}_f$, $\mathbf{b}_f$ and $\mathbf{c}_f$ are the loading vectors of the chromatographic, spectral and sample profiles, respectively, and e_{ijk} are the residuals of the model. The coordinates of the loading vectors are the columns of matrix $\mathbf{A}$, $\mathbf{B}$ and $\mathbf{C}$ of size $I \times F$, $J \times F$ and $K \times F$, respectively.

Data are trilinear if the experimental data tensor is compatible with the structure in Eq. (1). In this case, the estimation by least squares of all the coefficients that intervene in that equation is unique.

The core consistency diagnostic (CORCONDIA) [31] measures the trilinearity degree of the experimental data tensor. If the data tensor is trilinear, then the maximum CORCONDIA value of 100 is found.

PARAFAC model is highly affected by deviations from the trilinear structure. Shifts in the retention time of analytes from sample to sample often happen in chromatography and this could affect trilinearity. PARAFAC2 [32,33] is a slightly different decomposition technique that overcomes the inequality in the chromatographic profiles and allows some deviation in them:

$$\underline{\mathbf{X}} = \left(x_{ijk} \right) = \left(\sum_{f=1}^{F} a_{if}^{k} b_{jf} c_{kf} + e_{ijk} \right), \quad i = 1, 2, \ldots, I; \quad j = 1, 2, \ldots, J; \quad k = 1, 2, \ldots, K \tag{2}$$

where the superscript k is added to account for the dependence of the chromatographic profile on the kth sample. As a consequence, the loading matrices $\mathbf{A}_k$ are not necessarily

equal for all $k = 1,…,K$. So, while PARAFAC applies the same profiles (**A**, **B**) to a parallel set of matrices, as shown in Eq. (1), PARAFAC2 applies the same profile (**B**) along the spectral mode instead, allowing the chromatographic mode to vary from one matrix to another. The model in Eq. (2) does not have the uniqueness property. To obtain it, the cross-product, $\mathbf{A}_k^T$ $\mathbf{A}_k$, is restricted to be the same for $k = 1,…, K$. Details and bibliographical references related to this question can be seen in [34].

The identification of outlier samples can be done through the indices Q and Hotelling's T^2. If both indices of a sample exceed the threshold values at a certain confidence level, that sample should be rejected and the PARAFAC or PARAFAC2 model should be estimated again.

When PARAFAC and PARAFAC2 have the uniqueness property, the unequivocal identification of compounds is possible by their chromatographic and spectral profiles, as some official regulations and guidelines [21-23] state.

3.2. Comparison of regression models

The evaluation of possible matrix effects was conducted following the strategy proposed by [35,36]. Suppose that three calibration sets, namely C1, C2 and C3, on a response y and a predictor x are available, and that a linear least-squares (LS) fitting is to be carried out on each one of them. The comparison of those three lines at once to check if they can be described by the same mathematical model can be performed by posing the following regression equation

$$y = \beta_0 + \beta_1 x + \alpha_0 z_1 + \alpha_1 z_1 x + \alpha_2 z_2 + \alpha_3 z_2 x + \varepsilon \qquad (3)$$

being ε the independent, equal and normally distributed residual error. Two indicator variables, z_1 and z_2, appear in Eq. (3) to define the three separate functional models for C1, C2 and C3 by letting $z_1 = z_2 = 0$ in the first case, $z_1 = 1$ and $z_2 = 0$ in the second case, and $z_1 = 0$ and $z_2 = 1$ in the third case, respectively; that is,

C1 model function: $y = \beta_0 + \beta_1 x$ $\qquad (4)$

C2 model function: $y = \left(\beta_0 + \alpha_0\right) + \left(\beta_1 + \alpha_1\right) x$ $\qquad (5)$

C3 model function: $y = \left(\beta_0 + \alpha_2\right) + \left(\beta_1 + \alpha_3\right) x$ $\qquad (6)$

On the one hand, the coefficients α_0 and α_1, and α_2 and α_3 on the other hand, represent the changes needed to get from the C1 functional model to the C2 or the C3 one, respectively. So, if, after hypothesis testing, it is concluded that $\alpha_0 = \alpha_1 = \alpha_2 = \alpha_3 = 0$, it can thus be stated that the three models under comparison are the same.

This strategy to evaluate the equality of several calibration curves is of great application in chemical analysis, especially to check if matrix effects are present [37], which could

adversely affect both identification and quantification of analytes if not properly corrected [38]. In GC determinations, a matrix-induced chromatographic response enhancement effect often occurs: in solvent standards without sample matrix present, only the analytes fill the active sites in the system (injector, column, detector), which reduce the percentage of injected molecules eventually detected. However, in complex injected extracts, the active sites are filled predominantly by matrix components, thereby increasing efficiency of analyte transfer through the GC system to the detector [39]. For the study of the existence of matrix effects in this work, calibration set C2 was made up of matrix-matched standards, whereas C1 and C3 consisted of two arrays of standards of similar concentrations in the solvent. So two solvent calibration sets were selected to check the extent of the possible matrix effects by comparing the regression model estimated before (C1 set) and after (C3 set) analysing the matrix-matched standards (C2 set). The results obtained from this study are commented in Section 4.3.

4. Results and discussion

4.1. Validation of the analytical procedure

4.1.1 Unequivocal identification

The requirements laid down in EUR 24105 EN [21] for the unequivocal identification of the analytes were followed in this work. To establish the permitted tolerance intervals, six reference standards were prepared and analysed. Table 1 (first row) shows the concentration ranges of these standards. Three of them contained the IS at a fixed concentration and the analytes at three concentration levels, while the rest contained the IS at three concentration levels and the analytes at a fixed concentration. A solvent blank (only hexane) as well as three system blanks (no liquid) injected at the beginning, the middle and the end of these analyses were measured to test the performance of the GC/MS system. After baseline correction, the resulting ten chromatograms were equally fragmented around the retention time of each analyte and the fragments (data matrices) related to the same compound were arranged together into a data tensor $\underline{\mathbf{X}}$. The dimensions of these tensors are specified in Table 1 (first row, columns 4-8): it must be noticed that a joint array was built for DiBP and DiBP-d_4 peaks. A PARAFAC decomposition of each tensor was then performed as can be seen in Table 2. A one-factor unconstrained model was needed for BHT, BP and DEHA. The PARAFAC model for DiBP and the internal standard required three factors, being DiBP and DiBP-d_4 the first and second factors, respectively, while the third factor was an interferent that eluted before DiBP-d_4. The PARAFAC model for DiNP also needed three factors. These PARAFAC decompositions provided the unique chromatographic and spectral profiles of every compound that is common to all the samples. Therefore, the retention time for each analyte obtained through the chromatographic profile enabled to calculate the tolerances for its relative retention time (the ratio of the chromatographic retention time of the analyte to that of the internal standard), which appears in the fourth column of Table 2. The tolerance intervals for the relative retention time of all the analytes are collected in the fifth column of this table. In the case of DiNP, it was not possible to establish its retention time since finger peaks appeared

in its chromatogram. In addition, the spectral loadings were used to calculate the relative abundances of each m/z ion with regard to the base peak and thus determine the tolerance intervals for the relative ion abundances (see Table 2, columns 6-9). Both kinds of intervals would be now used as reference to confirm the presence of the corresponding compound in every sample.

4.1.2 Calibration

Twelve calibration standards were prepared within the concentration ranges detailed in Table 1 (second row) and analysed in duplicate. The ubiquity of DiBP in the previously analysed solvent blanks made its quantification impossible because this analyte appeared in a different quantity in each solvent blank injected. So, the concentration of DiBP was fixed at 25 µg L^{-1} in these calibration standards, which is below the generic SML. To carry out the calibration based on PARAFAC, the data tensors were built with these standards together with 8 system blanks, a solvent blank without IS and 22 solvent blanks with IS. The dimensions of these three-way tensors are given in Table 1 (second row) for each analyte, while the features of the model estimated from the PARAFAC decomposition of each tensor are included in the second column of Table 3.

For all the analytes, it was checked if their relative retention times obtained through the chromatographic profile and the relative abundances calculated with the loadings of the spectral profile for each diagnostic ion (see the third column of Table 3) were within the corresponding tolerance intervals established previously (see Table 2). Only the relative abundance of the m/z ratio 57 for DiNP lay outside its corresponding tolerance interval. However, 5 m/z ratios met the identification conditions for this analyte. So, it could be stated that the presence of all compounds was unequivocally confirmed.

Once the sample loadings for each analyte had been standardized by dividing each of them by that of the internal standard, calibration lines "standardized sample loading *versus* true concentration" were performed with the 24 standards. Table 3 (fourth column) shows the parameters of the LS regression models estimated for each analyte. A second-degree polynomial model was considered for BP and DiNP since a lack of fit was concluded in the linear model at 95% confidence level. The regression models were significant in all cases and no outlier data were detected. The highest mean of the absolute value of the relative errors in calibration was 6.71% (n = 22) for DEHA, while the lowest value was obtained for DiNP: 2.32% (n = 22). In addition, the intercept of the corresponding accuracy line ("estimated concentration *versus* true concentration", see the equations in the sixth column of Table 3) was equal to 0 and its slope was equal to 1 at a significance level of 5% in all cases. Therefore, trueness was verified for all the analytes at 95% confidence level. The decision limit (CCα) and the detection capability (CCβ) values are also contained in the two last columns of Table 3. The CCβ values were: 2.3 µg L^{-1} for BHT, 2.7 µg L^{-1} for BP, 3.6 µg L^{-1} for DEHA and 101.7 µg L^{-1} for DiNP (for α = β = 0.05 and two replicates). The details of the procedure to obtain CCβ from three-way data can be found in [40].

By way of example, Fig. 1 shows the total ion chromatogram (TIC) of the calibration standard injected at the highest concentration. As can be seen in this figure, finger peaks appeared in the chromatogram for DiNP because of an array of possible C_9 isomers, as

commented in Section 1. Therefore, it was not possible to establish a retention time for this analyte, as can be seen in Tables 2 and 3. In addition, this analyte appeared as a broad peak, which took about 2 min to elute (see Fig. 1). This is the reason why a big number of scans (823) was considered for this analyte in this work (see Table 1, column 8).

The quantification of DiNP is usually performed on the sum of peak areas corresponding to the different isomers [41]. But, as the signal for this analyte has such a complex shape, the results could vary significantly depending on the skill and experience of the chromatographist. However, a more accurate choice, namely, a calibration based on PARAFAC for this special case was used in this work, as explained previously. Fig. 2 shows the loadings of the PARAFAC decomposition of the tensor **X** (823 × 6 × 55) built for DiNP in the calibration step (see its features in Table 3). The loadings of the chromatographic profile (Fig. 2(a)) for the factor identified as DiNP showed its typical finger peaks, whereas the ones for the second factor (the baseline) decreased with the elution time. So, there was still baseline together with this analyte although a previous correction had been made for those chromatograms. In Fig. 2 (b), it can be observed that the m/z ratio 57 was characteristic of the baseline and shared with DiNP. The m/z ratio 149 was the base peak for DiNP like in most EI spectra of phthalates. The loadings of the sample profile (Fig. 2 (c)) for DiNP increased with the concentration of the calibration samples, whereas they were zero for the system and solvent blanks (blue circles near zero). However, the sample loadings of the baseline factor remained nearly constant for the calibration and blank samples and these values were higher than the ones for the system blank samples (sample numbers 1, 2, 16, 23, 32, 41, 50 and 55, red circles near zero). So, this PARAFAC model was coherent with the experimental knowledge and the calibration results for this analyte were satisfactory. Therefore, it can be concluded that PARAFAC succeeded in the determination of DiNP since no peak areas but loadings were considered. As far as the authors are aware, this is the first time PARAFAC has been used to deal with finger-peak chromatographic signals.

4.2. Ubiquity of DiBP in the laboratory: strategy to assess if the amount of DiBP present in a sample is higher than the blank level

As previously mentioned, a changeable presence of DiBP was observed from the first stages of this work, even when solvent blanks were analysed. This fact did not allow the quantification of this compound to be carried out by means of a regression line, because its blank concentration varied significantly over time, even throughout a routine analytical sequence. Therefore, a proper calibration model could not be estimated without having assessed that blank level properly first.

Despite this, as commented in Section 1, a comparison between the probability distributions of the level of DiBP in solvent blanks and in solvent standards at a fixed concentration could be made. The probability distribution related to the amount of DiBP in solvent blanks would account for the non-constant pattern of this analyte in the laboratory environment. That comparison would be posed through a hypothesis test; the critical value of the standardized sample loading of DiBP beyond which the concentration of this analyte in a solvent standard

would be statistically greater than that in the laboratory environment could be estimated after setting the values of the α and β errors that would be taken.

4.2.1 Data structure

To estimate the two probability distributions for this study, 50 solvent blanks on the one hand and 44 solvent standards with 25 µg L^{-1} of DiBP on the other hand were analysed, both sets containing DiBP-d_4 at 25 µg L^{-1}. The number of objects in each distribution was selected to prevent the insensitivity of the goodness-of-fit hypothesis tests. According to [42], for the Kolmogorov-Smirnov test, letting the distance between the two experimental distributions be 0.3 at the most, a size of about 50 objects must be considered for each distribution in order to ensure that the power of the test is 90%. The rest of the analytes were also included in these solvent standards to avoid significant differences in the signals of DiBP and DiBP-d_4 due to the absence of some compounds in the GC liner. Otherwise, it may result in a different adsorption/evaporation behaviour of DiBP and DiBP-d_4 in the inlet, which could lead to results and conclusions that may not be statistically comparable to those obtained in other steps of this work. The concentration ranges of BHT, BP, DEHA and DiNP in these standards are listed in Table 1 (third row).

Besides the assessment on the blank amount of DiBP, another study was carried out in parallel. Some rubber latex nipples used to make up the reference standard solutions to the calibration mark of the flask were suspected of being one of the sources of cross-contamination of DiBP. To test that and the possible leaching of the other four compounds from the polymer, two different nipples (referred as N1 and N2) were used to pipette hexane into 5-mL flasks to prepare solvent blanks; the IS at a final concentration of 25 µg L^{-1} had been previously added. Four situations during this stage were simulated, each in duplicate (replicates referred as R1 and R2): on the one hand, solvent (hexane) was not allowed to reach up and be in contact with the nipple polymer (samples named as N1_0_R1 and N1_0_R2 for nipple N1, while N2_0_R1 and N2_0_R2 for nipple N2), and on the other hand, there were one, two and three forced contacts, respectively (samples named as N1_1_R1 and N1_1_R2, N1_2_R1 and N1_2_R2, N1_3_R1 and N1_3_R2 for nipple N1 at each of these three situations; the same code was used for the blanks from nipple N2). So a total of 16 solvent blanks prepared in this way resulted, eight for each nipple.

In addition to the 50 solvent blanks and the 44 solvent standards for the study on DiBP and the 16 nipple blanks, both system blanks and solvent blanks without IS were injected to control the performance of the GC/MS equipment. It must be pointed out that no nipples were used in the volume adjustment of any solutions, except for those specifically indicated, either in this stage of the work or in the following. Because of the impossibility to carry out the resulting 130 analyses within the same day, the sequence was performed in two days (55 analyses on the first day, 75 analyses on the second one). After background subtraction, five data tensors whose dimensions are collected in Table 1 (third row) were built.

4.2.2 Data analysis

The PARAFAC decomposition of the tensor related to BHT showed the existence of one single factor unequivocally linked to this analyte (no constraints imposed, explained variance of 99.59%, no outliers detected regarding the threshold values at 99% confidence of Q and T^2 indices).

An unconstrained one-factor model was also obtained for BP (explained variance of 92.41%, no outliers), whose presence was also guaranteed in terms of retention time and mass spectrum.

As for the joint three-way tensor for DiBP and DiBP-d_4, its PARAFAC decomposition yielded a three-factor model (CORCONDIA of 98 %, explained variance of 98.90%, 11 outliers finally removed), where the chromatographic and spectral ways had been non-negativity-constrained. Factor 1 in this model (in dark blue in Figs. 3a, 3b and 3c) was unequivocally associated to DiBP and factor 2 (in light green in Figs. 3a, 3b and 3c) was to DiBP-d_4, whereas factor 3 (in red in Figs. 3a, 3b and 3c) was considered an unidentified interferent eluting near the beginning of the DiBP-d_4 peak. Fig. 3c reveals that the sample loadings of DiBP for the nipple blanks were higher than those for solvent blanks, so the suspicions about the leaching of DiBP out from the nipples evaluated were reasonable.

On the other hand, Figs. 4a (solvent blanks) and 4b (solvent standards at 25 µg L^{-1}) display the values of the standardized sample loadings of DiBP for the two sets under study. It can be seen that, although greater values of the sample loadings of both DiBP and especially DiBP-d_4 were obtained on the second day of analysis (see blue and green circles in Fig. 3c), the standardization procedure succeeded in compensating for the variations responsible for that shift.

The 11 outliers detected in the tensor for DiBP and DiBP-d_4 that contained the initial 130 samples corresponded to 10 nipple blanks and 1 system blank; to be precise, as Figs. 5a and 5b show, only the four solvent blanks where hexane had had no contact with the nipple (samples N1_0_R1, N1_0_R2, N2_0_R1 and N2_0_R2, which correspond to sample numbers 113, 114, 115 and 116, respectively, in Fig. 3c) and those prepared after 1 contact of hexane with nipple N2 (samples N2_1_R1 and N2_1_R2; sample number 117 and 118 in Fig. 3c) could not be considered outliers. The rest of the nipple blanks lay out of the plane defined by the threshold values of Q and T^2 indices at 99% confidence level; this meant that all these outliers were placed far away both from the new space spanned by the three factors of the PARAFAC model in the sample mode and from the centroid of the samples. By having a close look at Fig. 5a, the values of Q and T^2 indices for the nipple blanks revealed important differences among these samples, being each class of nipple blanks (regarding the number of contacts with hexane) located separately in the plot. This was confirmed by the fact that no constant values of the sample loadings of DiBP-d_4 were obtained for the 16 nipple blanks: the higher the number of contacts between hexane and the nipple polymer, the greater the sample loading of the IS, as shown in Fig. 3c when comparing the results for the 0-contact blanks (sample numbers 113 to 116) and those for the 1-contact blanks for nipple N2 (sample numbers 117 and 118). This fact could be responsible for those outlier nipple blanks to be different from the rest of the samples in the tensor in terms of Q and T^2 values, and led to think of the possibility of matrix effects that would account for the signal enhancement observed throughout the analysis of the nipple blanks. This hypothesis is assessed in Section 4.3.

Regarding DEHA, a two-factor PARAFAC model was estimated (CORCONDIA of 100 %, explained variance of 98.62%, no outliers found) after a non-negativity constraint had been laid down on the chromatographic, spectral and sample ways. Factor 1 matched DEHA unequivocally, whereas factor 2 was attributed to an unknown interferent that mainly eluted in the nipple blanks.

Lastly, the PARAFAC decomposition of the DiNP tensor revealed, through a two-factor non-negativity constrained model (CORCONDIA of 100 %, explained variance of 98.73%, no outliers rejected), that the baseline signal (factor 2) could be totally set apart from the chemical information on DiNP (factor 1), which enabled its unequivocal identification.

Fig. 6 depicts the values of the standardized sample loadings of the five analytes in the 50 solvent blanks, the 44 solvent standards and the 6 nipple blanks eventually considered. It is clear from this plot that BP, DEHA and DiNP were not found either in the solvent blanks (no evidence of the presence of these three compounds in the lab environment) or in the nipple blanks (no leaching of these substances from the polymer). As for BHT, a slightly amount of this analyte seemed to appear on both solvent and nipple blanks, but displaying a uniform pattern: in fact, the values of the standardized sample loadings for BHT in both kinds of blanks varied between 0.09 and 0.12, being the mean and the standard deviation equal to 0.09 and 0.02, respectively. The concentration of BHT corresponding to that mean value was determined from the regression line "standardized sample loading *versus* true concentration" estimated in the study in Section 4.1. As the result was -0.06 ± 1.91 µg L^{-1}, it could be concluded that BHT was not present in the lab environment and did not leach out of the nipple polymer either, because its blank concentration after both studies was statistically equal to 0. However, as pictured in Fig. 6, the situation for DiBP was quite different, since non-zero standardized sample loadings were obtained for both solvent and nipple blanks; furthermore, as stated above, due to the variations in those values, the estimation of a trustworthy calibration line was not possible, and the strategy based on the assessment of the probability distributions was thus designed.

The distributions coming from the two classes, namely, distribution 1 for the solvent blanks and distribution 2 for the solvent standards at 25 µg L^{-1}, were compared by means of a Kolmogorov-Smirnov test (H$_0$: Distribution 1 = Distribution 2; H$_a$: Distribution 1 ≠ Distribution 2), which is performed by computing the maximum distance between the cumulative distributions of the two sets. Since the p-value for this test was 4.5 10^{-9}, it could be concluded that there was a statistically significant difference between the two distributions at 95% confidence level. That is, both data sets could not be modelled by the same type of probability density function, which meant that the pattern of DiBP was completely different at these two concentration levels. The standardized sample loadings from the solvent blanks (distribution 1) could not be adequately fitted to a normal distribution, but to a 3-parameter lognormal one with mean 0.43, variance 0.03 and lower threshold 0.23. However, the data from the solvent standards (distribution 2) were contrasted to follow a normal distribution N(1.37, 0.02). The plot of both distributions is shown in Fig. 7a.

To decide when the amount of DiBP in a sample could be considered as statistically different (greater) than that at the blank level, a hypothesis test was posed on these two probability distributions. This situation was formally expressed as

H_0: DiBP is present at the blank amount; that is, the sample comes from distribution 1   (7)

H_a: DiBP is present at an amount greater than that in the laboratory environment; that is, the sample comes from distribution 2   (8)

The critical standardized sample loading of DiBP that would mean the lowest value of this variable beyond which the null hypothesis H_0 would be rejected was computed after having specified the probabilities of false non-compliance (α) and of false compliance (β) taken when making a decision on this issue. α and β values are not independent, but change in opposite directions, as can be seen in Fig. 7b, where the operating-characteristic curve of this hypothesis test is displayed. From all the pairs (α,β) drawing this curve, the situation when $\alpha = \beta = 0.012$ was selected (marked with a yellow triangle in Fig. 7b), since the probabilities of making a type I error (α) and a type II error (β) were both low and equal. The critical value (standardized sample loading) of DiBP associated was 1.04, which is also represented in Fig. 7a with a dotted vertical line. This means that any sample, after performing PARAFAC or PARAFAC2 and confirming the presence of DiBP unequivocally, that has got a standardized sample loading of this analyte higher than 1.04 will contain DiBP in an amount significantly greater than that considered as blank in the laboratory environment, being the probabilities α and β equal to 0.012.

As for the amount of DiBP released from the nipples into the six remaining solvent blanks once outliers had been rejected, only samples N2_1 (replicates R1 and R2) were concluded to have DiBP at a level higher than the blank one, since their standardized sample loadings were 1.75 and 1.78, respectively. On the contrary, the values of this variable ranged from 0.25 to 0.30 for the four nipple blanks prepared without allowing any contacts between the nipple polymer and hexane.

4.3. Evaluation of possible matrix effects

The existence of matrix effects on the GC signals due to the presence of sample matrix when injecting the blanks prepared from nipples was assessed. The nipple that showed the highest level of DiBP released in the previous stage, namely, nipple N1 (see Fig. 5a), was selected to perform this study. The calibration models estimated for the five analytes from three calibration sets were compared. One of them was made up of matrix- matched standards prepared by simulating two contacts of liquid hexane with the nipple during preparation; from the four concentration levels considered for the standards, the three of them different from zero were prepared and analysed in duplicate, whereas six blanks were prepared. The other two calibration sets consisted of solvent standards at the same concentration levels and with the same number of replicates as the matrix-matched series. These two solvent-standard sequences were analysed before and after the matrix-matched one, respectively, to test the extent of the possible matrix effects. The concentration ranges considered are specified in Table 1 (fourth row). A calibration model could be estimated for DiBP this time, since the lowest standard prepared for this study was at 25 µg L^{-1}, which had

been proved to be statistically different from the blank concentration ($\alpha = \beta = 0.012$) in the previous stage of the work (see Section 4.2).

After GC/MS analysis, five data tensors, each for every analyte, were built from all these standards, together with solvent and system blanks without containing IS, as it appears in Table 1 (fourth row); as ever, the data from DiBP and the IS were included in the same array. The features of the model estimated from the PARAFAC (or PARAFAC2) decomposition of every tensor are listed in Table 4 (second column). By comparing the chromatographic and spectral profiles of the factor associated to every analyte with those used as reference (see Table 2), it could be stated that all compounds were unequivocally identified.

As can be seen in Table 4, peak shifts forced to a PARAFAC2 decomposition of the array for DiBP and DiBP-d_4. The loadings in the third way (sample profile in this work) of a PARAFAC2 model are always obtained without being normalized, so the division of the sample loading vector of every factor by its norm had to be done prior to standardization and quantification.The equations of the LS regression models and the accuracy lines related to the three calibration sets analysed are also collected in Table 4 (columns 3-8). The criterion used for considering a sample as an outlier in every set with regard to the regression model was to have a studentized residual greater than 3 in absolute value. Trueness was verified in all cases at 95% confidence level.

As explained in Section 3.2, the possible matrix effects in the determination of the five analytes in the nipple extracts were assessed by checking the statistical equality of the three calibration models "standardized sample loading *versus* true concentration" estimated. The model in Eq. (3) was fitted to the experimental data from the three sets just for BHT, DEHA and DiNP. For BP and DiBP, different mathematical functions (quadratic instead of linear models) were obtained for the solvent calibration curves and for the matrix-matched calibration (see Table 4), since a significant lack of fit was found when a linear regression was posed; this fact confirmed that the quantification of BP and DiBP in the nipple samples was affected by the presence of matrix components: the analytical behavior of each of these two compounds was described by different functional models (polynomial instead of linear regressions) depending on the environment where they were in solution.

For BHT, DEHA and DiNP, once the model in Eq. (3) had been fitted in each case, the hypothesis test on the statistical significance of the estimated coefficient of every term including the indicator variables z_1 and z_2 was posed, where H_0: $\alpha_i = 0$ *versus* H_a: $\alpha_i \neq 0$; the resultant p-values are shown in the last column of Table 4. At 99% confidence level, some of the estimates of α_0, α_1, α_2 and α_3 were significantly non-null for those three analytes. As a consequence, the analytical sensitivity of every analyte was different, so matrix effects were also proved to be present for BHT, DEHA and DiNP. These joint matrix problems detected for the five compounds under study led to the decision of performing their quantification in future studies following the standard addition method.

4.4. Extraction from a dummy

A dummy made of natural rubber latex was purchased from a local supermarket. An extraction from this dummy into hexane was carried out as detailed in Section 2.3.

The standard addition method was used to determine the concentration of the analytes studied in this work in the sample, as explained above. Each analyte was added within the concentration ranges included in Table 1 (fifth row). For the special case of DiBP, the lowest added concentration was 25 µg L^{-1} since the procedure to assess the level of this analyte in solvent blanks (explained in Section 4.2) was done at this concentration level.

High amounts of BHT were detected in the extracted solution, so it was necessary to perform the standard addition method twice. The first one was carried out using 4.5 mL of the extracted solution into 5 mL volumetric flasks (with 25 µg L^{-1} of DiBP-d$_4$) in order to quantify BP, DiBP, DEHA and DiNP. However, as the quantity of BHT present was too high, the second one was performed to quantify only BHT. In this case, the extract was more diluted (1.3 mL of the same extracted solution into 5 mL volumetric flasks) and contained a higher amount of the internal standard (225 µg L^{-1} of DiBP-d$_4$) than in all the previous stages of this work.

In both analyses, seven matrix-matched standards at seven concentration levels were injected in duplicate. All the analytes were added to these standards (except for the first one), although only some of them would be quantified in each case. The concentration levels of each analyte in both analyses were the same except for BHT, since its concentration range was reduced for the development of the first standard addition regression (0-30 µg L^{-1}). One solvent blank without IS was also injected at the beginning of both analytical sequences and a system blank was analysed between each matrix-matched standard.

A three-way data tensor containing all the data from the first standard addition set was built for BP, DiBP (with DiBP-d$_4$), DEHA and DiNP, while only data tensors for BHT and the internal standard (DiBP-d$_4$) were built for the second one. The dimensions of these data tensors are specified in Table 1 (fifth row), whereas the characteristics of the PARAFAC decompositions performed for each tensor are collected in Table 5.

The PARAFAC decomposition for BHT and BP required just one factor. In the case of DiBP-d$_4$, a three-factor PARAFAC2 model was needed for the data obtained from the first performance of the standard addition method. The first factor was the interferent that eluted before the internal standard as explained in previous sections; the second factor was associated with DiBP-d$_4$ and the third one with DiBP. On the other hand, when the PARAFAC decomposition of the tensor containing DiBP-d$_4$ for the quantification of BHT was performed, a two-factor model that was coherent with the presence of DiBP and DiBP-d$_4$ was obtained.

The PARAFAC decomposition of the DEHA tensor yielded a three-factor model where two interferents coeluted in the matrix-matched standards, while a three-factor PARAFAC2 model was necessary for DiNP. In this last case, the first factor was associated to an interferent that appeared mainly in the system blanks, the second factor was associated to DiNP and the third one was the baseline.

By way of example, the sample loadings for BHT are represented in Fig. 8. There was not a memory effect since the sample loadings for all the system blanks had a null value. The sample loading for the first matrix-matched standard and its replicate (in which only the internal standard had been added) was different from zero as expected. The loadings for the remaining matrix-matched standards were in increasing order, which was coherent.

It must be taken into account that the GC column was cut due to maintenance tasks before the analysis of the samples corresponding to this section. This led to a variation in the absolute retention times regarding the ones obtained with the reference standards. However, there was no problem in the identification of each analyte since the relative retention times obtained in this section for each analyte (see Table 5, third column) lay within the tolerance intervals established previously (see Table 2). In addition, the unequivocal identification of each analyte was guaranteed since at least the relative abundances of 3 m/z ratios for each analyte (see Table 5, third column) were within their tolerance intervals (see Table 2).

The sample loadings of each analyte were standardized with the sample loadings of DiBP-d_4 obtained with the model required in each case. As commented in Section 4.3, the sample loadings of DiBP-d_4, DiBP and DiNP obtained with the data from the first performance of the standard addition method were numerically high because they came from PARAFAC2 decompositions, so they had to be manually normalized prior to standardization. Next, a LS regression between the standardized sample loadings of every analyte and the added concentration was built. All the regressions were significant and there was not a lack of fit in any case after the removal from the calibration set of the last matrix-matched standard and its replicate for BHT and DiNP and the two last ones and their replicates for DiBP. The parameters of the regression models built for each analyte and the results of this analysis are included in Table 5. The trueness of the method was verified for all analytes at 95% confidence level.

The amount of each analyte released from the dummy in the total volume of hexane together with the corresponding confidence interval are listed in Table 5. The concentration found for BP was below its CCα, the value obtained for DiBP was below the first standard fixed at 25 µg L^{-1}, so it could not be exactly determined, while the confidence interval for DEHA and DiNP contained zero. Therefore, BP, DEHA and DiNP were not detected in the extracted solution, while the exact concentration of DiBP could not be estimated. The conclusion reached after this study was that the presence of BHT from the dummy was observed.

4.5. Future developments

This work presents a methodology to face the two problems posed, but several issues still remain open. Regarding the unequivocal identification of every compound, one of them is that related to the retention time of finger-peak analytes like DiNP, so a strategy for the estimation of this feature or a similar one for complex signals is needed and currently being devised, as the relative retention time is one of the requirements that must be fulfilled at the identification step. On the other hand, the procedure to assess the blank level of DiBP permits its performance by considering a lower concentration of this analyte in the solvent standards for the distribution 2. Of course, both α and β would increase, but they would achieve quite good values anyway, as the results yielded for them in our work were low enough to achieve still low α and β errors even if the blank level of DiBP and the concentration value considered to pose the alternative hypothesis in the test were closer.

5. Conclusions

In the multiresidue determination of BHT, BP, DiBP, DEHA and DiNP by GC/MS, using DiBP-d_4 as internal standard, PARAFAC has succeeded in the unequivocal identification of every compound according to the performance requirements laid down in the EU legislation in force. Besides, this chemometric tool has offered an improved way to deal with complex finger-peak signals such as that of DiNP by using loadings instead of integrated areas in both identification and quantification steps.

The problem of the ubiquity of DiBP has also been overcome thanks to the statistical comparison of the two probability distributions of the level of this analyte in solvent blanks and standards and the assessment of the α and β errors taken. This has enabled to state that any standardized sample loading of DiBP significantly greater than 1.04 will indicate that this analyte is present in that sample at a concentration higher than that in blanks ($\alpha = \beta = 0.012$).

The evidence of matrix effects has forced to quantify every analyte by means of the standard addition methodology after an extraction into hexane from a natural rubber latex dummy. BHT has been the analyte undoubtedly detected as a potential migrant from the dummy at a concentration significantly different from zero.

6. Acknowledgments

7. References

[1] Office of Environmental Health Hazard Assessment's (OEHHA) - Reproductive and Cancer Hazard Assessment Branch, Evidence on the Carcinogenicity of Diisononyl Phthalate (DINP), California Environmental Protection Agency, October 2013.

[2] P. Ventrice, D. Ventrice, E. Russo, G. De Sarro, Phthalates: European regulation, chemistry, pharmacokinetic and related toxicity, Environ. Toxicol. Pharmacol. 36 (2013) 88-96.

[3] J. Annamalai, V. Namasivayam, Endocrine disrupting chemicals in the atmosphere: their effects on humans and wildlife, Environ. Int. 76 (2015) 78-97.

[4] M. Wagner, J. Oehlmann, Endocrine disruptors in bottled mineral water: total estrogenic burden and migration from plastic bottles, Environ. Sci. Pollut. Res. 16 (2009) 278-286.

[5] E. Fasano, F. Bono-Blay, T. Cirillo, P. Montuori, S. Lacorte, Migration of phthalates, alkylphenols, bisphenol A and di(2-ethylhexyl)adipate from food packaging, Food Control 27 (2012) 132-138.

[6] M.D. Spillmann, M. Siegrist, C. Keller, M. Wormuth, Phthalate exposure through food and consumers' risk perception of chemicals in food, Risk Analysis 29 (2009) 1170-1180.

[7] B. Cavaliere, B. Macchione, G. Sindona, A. Tagarelli, Tandem mass spectrometry in food safety assessment: The determination of phthalates in olive oil, J. Chromatogr. A 1205 (2008) 137-143.

[8] M.R. Lee, F.Y. Lai, J. Dou, K.L. Lin, L.W. Chung, Determination of trace leaching phthalate esters in water and urine from plastic containers by solid-phase microextraction and gas chromatography–mass spectrometry, Analytical Letters 44 (2011) 676–686.

[9] A. Afshari, L. Gunnarsen, P.A. Clausen, V. Hansen, Emission of phthalates from PVC and other materials, Indoor Air 14 (2004) 120-128.

[10] C. S. Giam, H. S. Chan, G. S. Neff, Rapid and inexpensive method for detection of polychlorinated biphenyls and phthalates in air, Anal. Chem. 47 (1975) 2319-2320.

[11] Commission Regulation (EU) No 10/2011 of 14 January 2011 on plastic materials and articles intended to come into contact with food, Official Journal of the European Union, L 12, 1-89.

[12] A. Fankhauser-Noti, K. Grob, Blank problems in trace analysis of diethylhexyl and dibutyl phthalate: Investigation of the sources, tips and tricks, Anal. Chim. Acta 582 (2007) 353–360.

[13] M. Marega, K. Grob, S. Moret, L. Conte, Phthalate analysis by gas chromatography–mass spectrometry: Blank problems related to the syringe needle, J. Chromatograph. A 1273 (2013) 105-110.

[14] A. Reid, C. Brougham, A. Fogarty and J. Roche. An investigation into possible sources of phthalate contamination in the environmental analytical laboratory, Intern. J. Environ. Anal. Chem. 87 (2007) 125-133.

[15] K. Furtmann, Phthalates in surface water – A method for routine trace level analysis, Fresenius J. Anal. Chem. 348 (1994) 291-296.

[16] F. David, P. Sandra, B. Tienpont, F. Vanwalleghem, M. Ikonomou, in: C.A. Staples (Ed.), Phthalate Esters, Part Q (The Handbook of Environmental Chemistry, vol. 3), Springer-Verlag, Berlin, Heidelberg, 2003, pp. 9-56.

[17] M.C. Ortiz, L.A. Sarabia, M.S. Sánchez, Tutorial on evaluation of type I and type II errors in chemical analyses: From the analytical detection to authentication of products and process control, Anal. Chim. Acta 674 (2010) 123–142.

[18] M.C. Ortiz, L.A. Sarabia, M.S. Sánchez, A. Herrero, Quality of analytical measurements: statistical methods for internal validation, in: S. Brown, R. Tauler, R. Walczak (Eds.), Comprehensive Chemometrics, vol. 1, Elsevier, Oxford, 2009, pp. 17–76.

[19] European Union risk assessment report. 1,2-Benzenedicarboxylic acid, di-C8-10-branched alkyl esters, C9-rich and di-"isononyl" phthalate (DINP) CAS Nos: 68515-48-0 and 28553-12-0. EINECS Nos: 271-090-9 and 249-079-5. European Commission – Joint Research Centre, Institute for Health and Consumer Protection, European Chemicals Bureau (ECB). Volume 35 (2003).

[20] Plasticisers and Flexible PVC information centre. Available at: http://www.plasticisers.org/plasticisers/22/93/Diisononyl-phthalate-DINP (Accessed: 24/09/2015).

[21] Guidelines for performance criteria and validation procedures of analytical methods used in controls of food contact materials, first ed., 2009 (EUR 24105 EN).

[22] 2002/657/EC Commission Decision of 12 August 2002, implementing Council Directive 96/23/EC concerning the performance of analytical methods and the interpretation of results, Off. J. Eur. Commun. L 221 (2002) 8-36.

[23] SANCO/12571/2013, Guidance document on analytical quality control and validation procedures for pesticide residues analysis in food and feed, EU, Brussels, 2013.

[24] IARC Monographs – 101. Benzophenone, pp. 285-304. Available at https://monographs.iarc.fr/ENG/Monographs/vol101/mono101-007.pdf (Accessed: 22/10/2015).

[25] NIST Mass Spectral Search Program for the NIST/EPA/NIH Mass Spectral Library Version 2.0 a. (build July 1 2002). National Institute of Standards and Technology, Gaithersburg, USA, 2002.

[26] B.M. Wise, N.B. Gallagher, R. Bro, J.M. Shaver, W. Winding, R.S. Koch, PLS Toolbox 6.0.1, Eigenvector Research Inc., Wenatchee, WA, USA.

[27] MATLAB, version 7.12.0.635 (R2011a), The Mathworks, Inc., Natick, MA, USA.

[28] STATGRAPHICS Centurion XVI Version 16.1.05 (32 bit), Statpoint Technologies, Inc., Herndon, VA, USA, 2010.

[29] L.A. Sarabia, M.C. Ortiz, DETARCHI. A program for detection limits with specified assurance probabilities and characteristic curves of detection, Trends Anal.Chem.13 (1994)1-6.

[30] R. Bro, PARAFAC. Tutorial and applications, Chemom. Intell. Lab. Syst. 38 (1997)149-171.

[31] R. Bro, H.A.L. Kiers, A new efficient method for determining the number of components in PARAFAC models, J. Chemom. 17 (2003) 274-286.

[32] H.A.L. Kiers, J.M.F. Ten Berge, R. Bro, PARAFAC2—Part I. A direct fitting algorithm for the PARAFAC2 model, J. Chemom. 13 (1999) 275-294.

[33] R. Bro, C.A. Andersson, H.A.L. Kiers, PARAFAC2—Part II. Modeling chromatographic data with retention time shifts, J. Chemom. 13 (1999) 295-309.

[34] M.C. Ortiz, L.A. Sarabia, M.S. Sánchez, A. Herrero, S. Sanllorente, C. Reguera, Usefulness of PARAFAC for the Quantification, Identification, and Description of Analytical Data, in: A. Muñoz de la Peña, H.C. Goicoechea, G.M. Escandar, A.C. Olivieri (Eds.), Fundamentals and Analytical Applications of Multiway Calibration, Elsevier, 2015, pp. 37-81

[35] N.R. Draper, H. Smith, Applied Regression Analysis, 3rd ed., John Wiley and Sons, New York, 1998.

[36] M.C. Ortiz, M.S. Sánchez, L.A. Sarabia, Quality of analytical measurements: univariate regression, in: S. Brown, R. Tauler, R. Walczak (Eds.), Comprehensive Chemometrics, vol. 1, Elsevier, Oxford, 2009, pp. 127–169.

[37] M.L. Oca, L.A. Sarabia, A. Herrero, M.C. Ortiz, Optimum pH for the determination of bisphenols and their corresponding diglycidyl ethers by gas chromatography–mass spectrometry. Migration kinetics of bisphenol A from polycarbonate glasses, J. Chromatogr. A 1360 (2014) 23–38.

[38] A. M. Botero-Coy, J. M. Marín, R. Serrano, J. V. Sancho, F. Hernández, Exploring matrix effects in liquid chromatography–tandem mass spectrometry determination of pesticide residues in tropical fruits, Anal. Bioanal. Chem. 407 (2015) 3667–3681.

[39] H. Kwon, S.J. Lehotay, L. Geis-Asteggiante, Variability of matrix effects in liquid and gas chromatography–mass spectrometry analysis of pesticide residues after QuEChERS sample preparation of different food crops, J. Chromatogr. A 1270 (2012) 235-245.

[40] M.C. Ortiz, L.A. Sarabia, I. García, D. Giménez, E. Meléndez, Capability of detection and three-way data, Anal. Chim. Acta. 559 (2006) 124-136.

[41] M.S. Pascal Gimeno, S. Thomas, C. Bousquet, A.-F. Maggio, C. Civade, C. Brenier, P.A. Bonnet, Identification and quantification of 14 phthalates and 5 non-phthalate plasticizers in PVC medical devices by GC-MS, J. Chromatogr. B 949-950 (2014) 99-108.

[42] F.J. Massey, Jr., The Kolmogorov-Smirnov Test for Goodness of Fit, J. Am. Stat. Assoc. 253 (1951) 68-78.

FIGURE CAPTIONS

Fig. 1   Total ion chromatogram (TIC) obtained from the injection of a calibration standard containing 50 µg L^{-1} of BHT and BP, 25 µg L^{-1} of DiBP and DiBP-d$_4$, 80 µg L^{-1} of DEHA and 3000 µg L^{-1} of DiNP. Peak labels: 1, BHT; 2, BP, 3, DiBP and DiBP-d$_4$; 4, DEHA; 5, DiNP.

Fig. 2   Loadings of the: (a) chromatographic profile, (b) spectral profile, (c) sample profile of the PARAFAC model with two factors built with the data tensor of DiNP for the calibration step (blue: DiNP, red: baseline). (For interpretation of the references to colour in this figure legend, the reader is referred to the web version of the article).

Fig. 3   PARAFAC decomposition of the common tensor for DiBP and DiBP-d$_4$. Loadings of the (a) chromatographic, (b) spectral and (c) sample profiles of the resulting PARAFAC model; factor 1 (DiBP): dark blue; factor 2 (DiBP-d$_4$): light green; factor 3: red. The index of sample number 112 is indicated in Fig. 3c for an easier understanding of the text. (For interpretation of the references to colour in this figure legend, the reader is referred to the web version of the article).

Fig. 4   Standardized sample loadings of DiBP for the solvent blank class (a) and the solvent standard class (b). (For interpretation of the references to colour in this figure legend, the reader is referred to the web version of the article).

Fig. 5   (a) Plot of the indices Hotelling's T^2 *versus* Q of the 119 samples that make up the joint tensor for DiBP and DiBP-d$_4$; the nipple blanks are marked in red triangles, while the rest of the samples are in grey circles. (b) Enlargement of Fig. 5a to show the threshold values of Q and Hotelling's T^2 at 99% confidence level (in dashed blue lines). (For interpretation of the references to colour in this figure legend, the reader is referred to the web version of the article).

Fig. 6   Values of the standardized sample loadings of the five analytes. BHT: light blue diamonds; BP: red squares; DiBP: light green triangles; DEHA: yellow circles; DiNP: black asterisks. (For interpretation of the references to colour in this figure legend, the reader is referred to the web version of the article).

Fig. 7   (a) Frequency histogram and probability distribution for the two sets under study: solvent blanks (distribution 1, in magenta) and solvent standards at 25 µg L^{-1} of DiBP (distribution 2, in black). (b) Operating-characteristic curve of the hypothesis test H$_0$: *The sample comes from distribution 1* against H$_a$: *The sample comes from distribution 2*. The values of the α and β errors finally considered are represented by the point marked with a yellow triangle. (For interpretation of the references to colour in this figure legend, the reader is referred to the web version of the article).

Fig. 8   Loadings of the sample profile of the one-factor PARAFAC model for the data tensor of BHT built with the samples analysed during the second performance of the standard addition method.

Figure 1

Fig. 1

Figure 2

(c)

Fig. 2

Figure 3

Fig. 3

Figure 4

Fig. 4

Figure 5

Fig. 5

Figure 6

Fig. 6

Figure 7

(a)

CRITICAL REGION

(b)
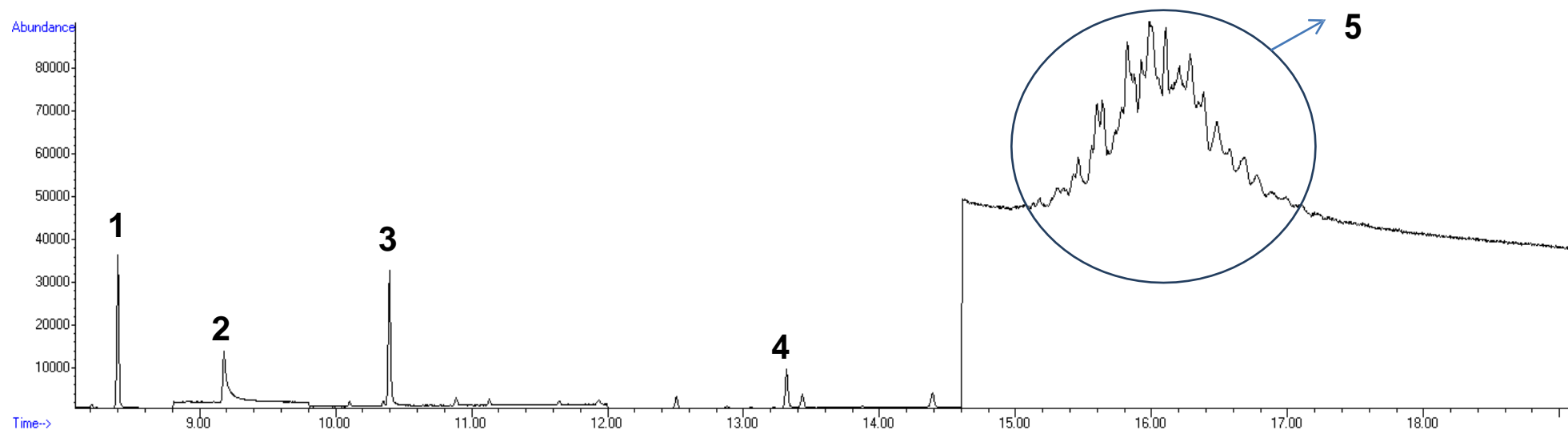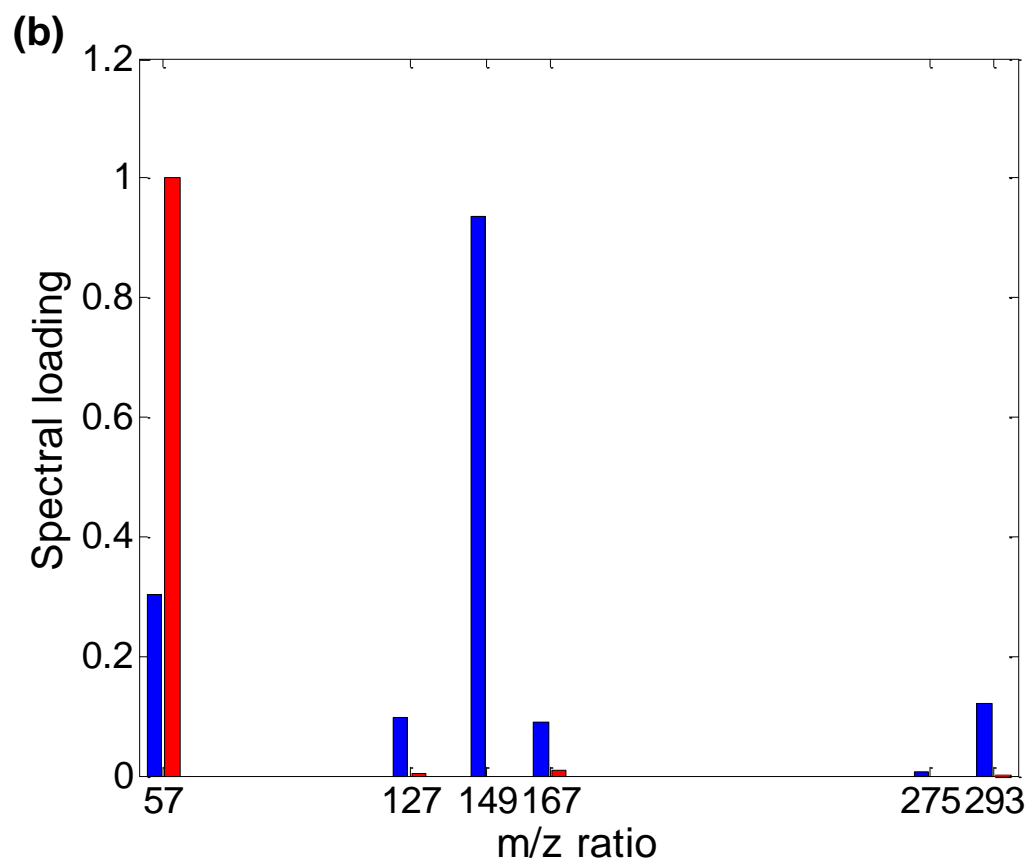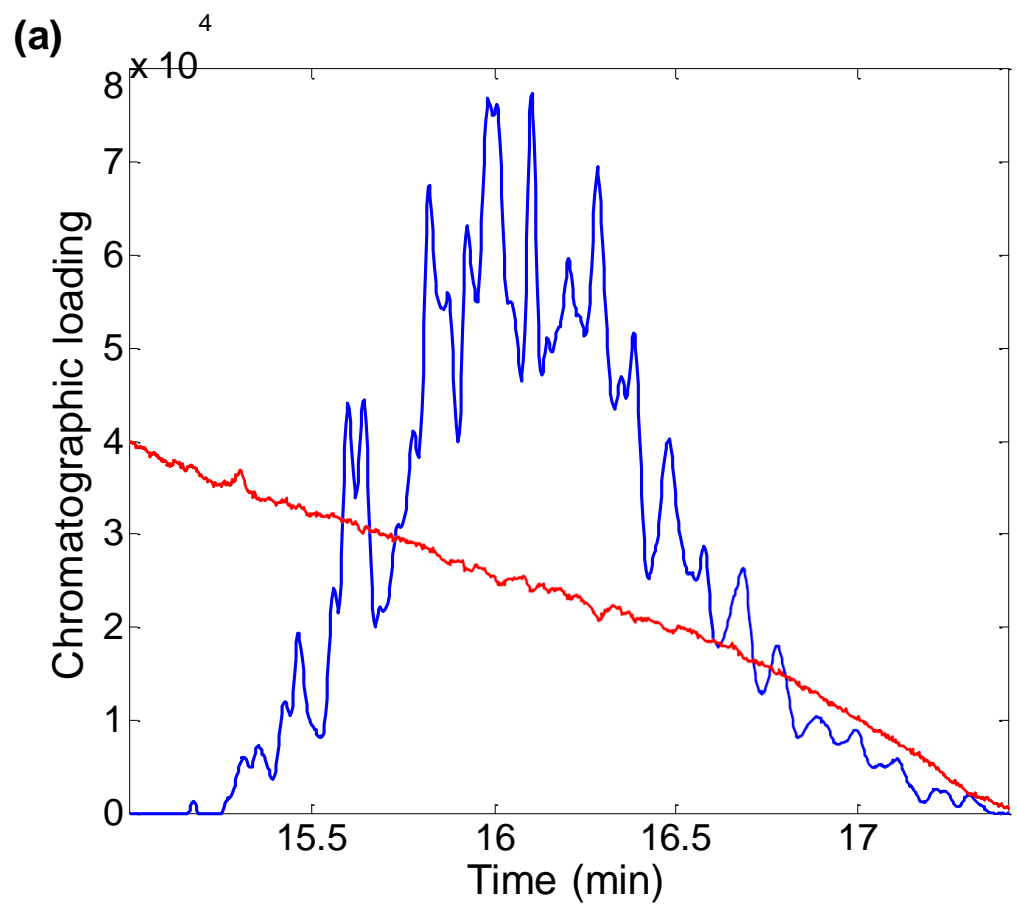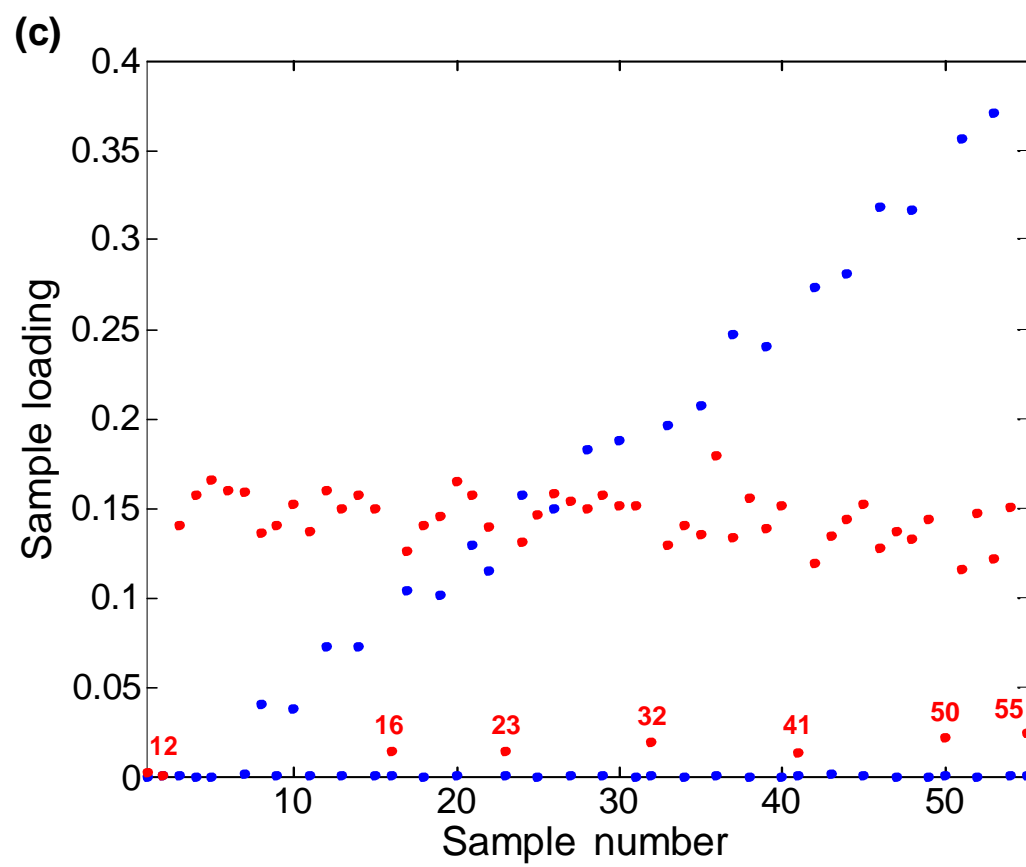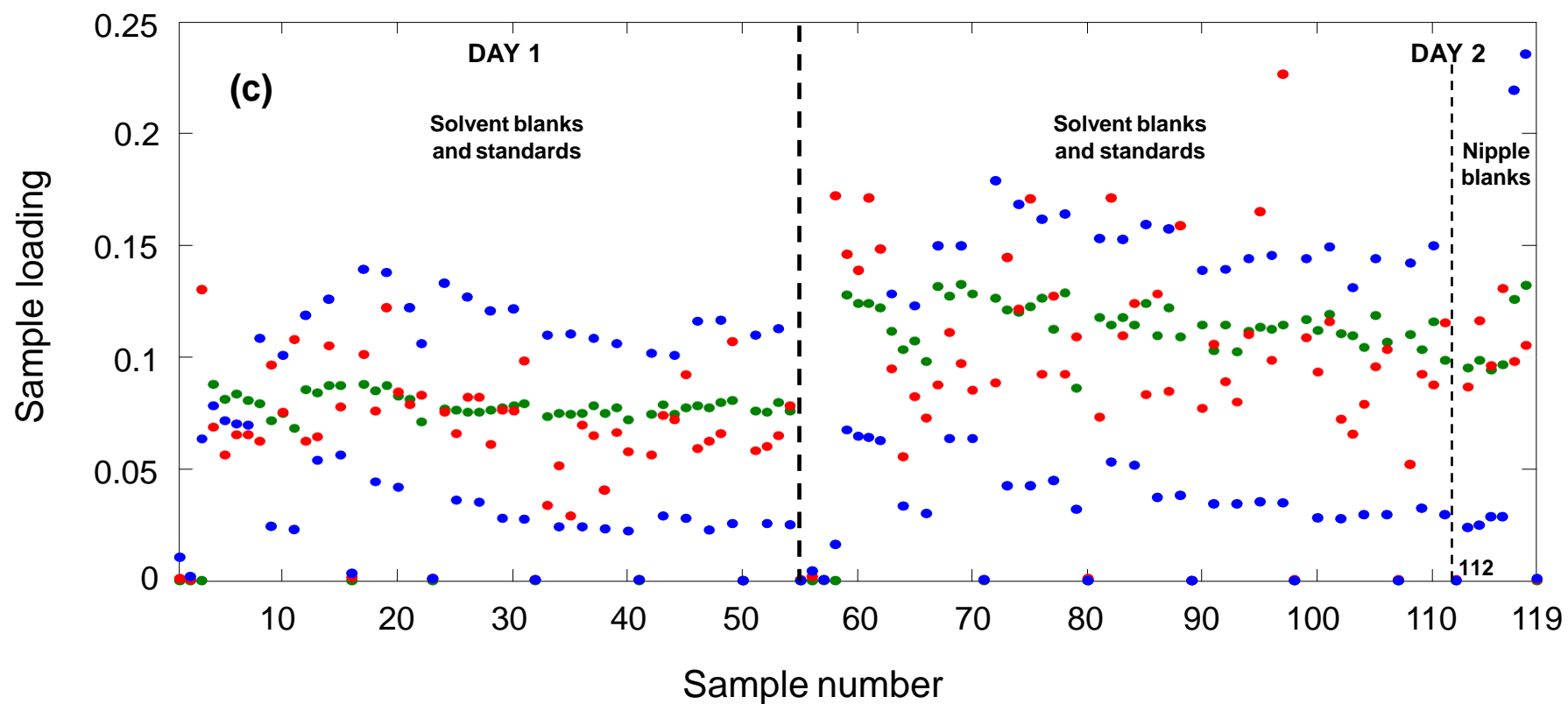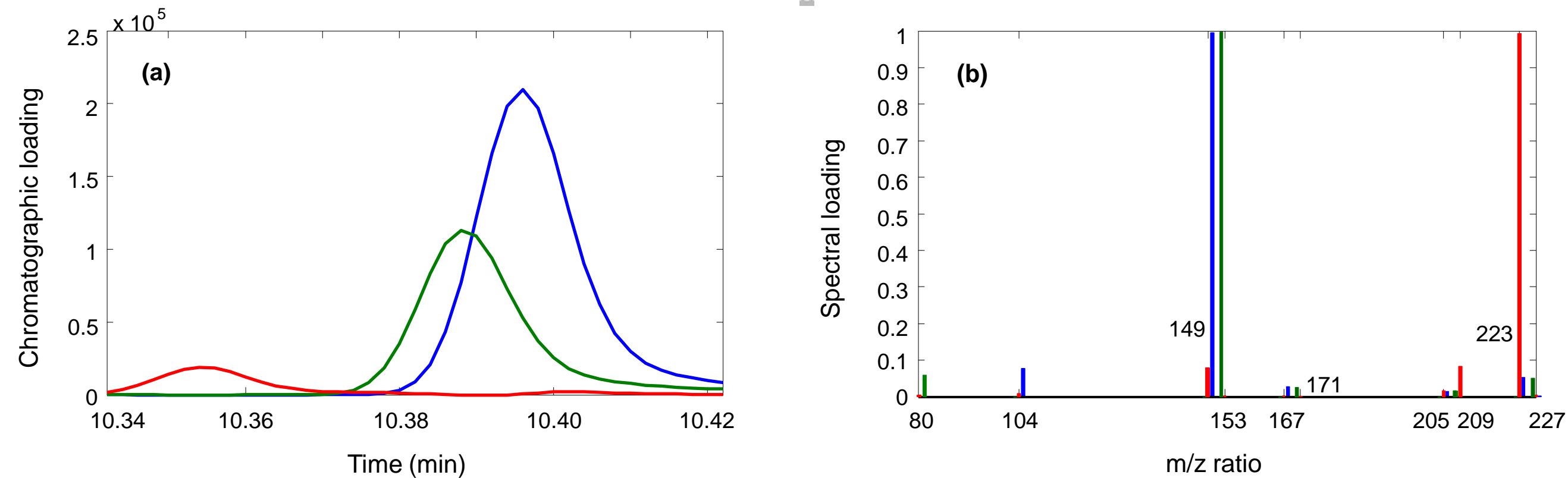
Fig. 7

Figure 8
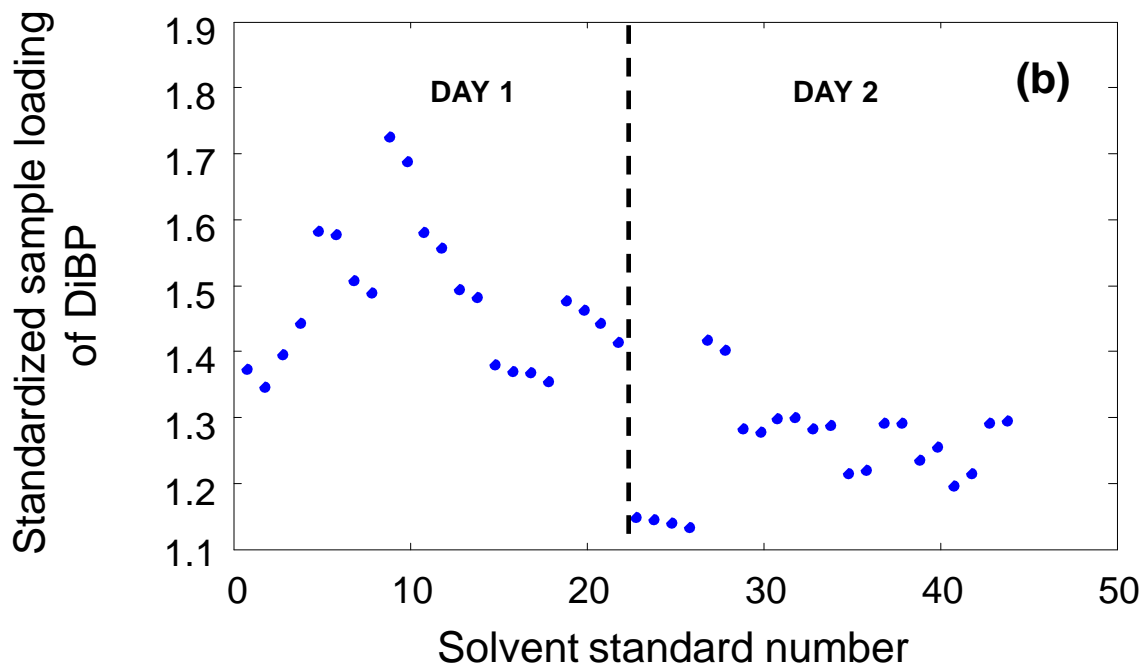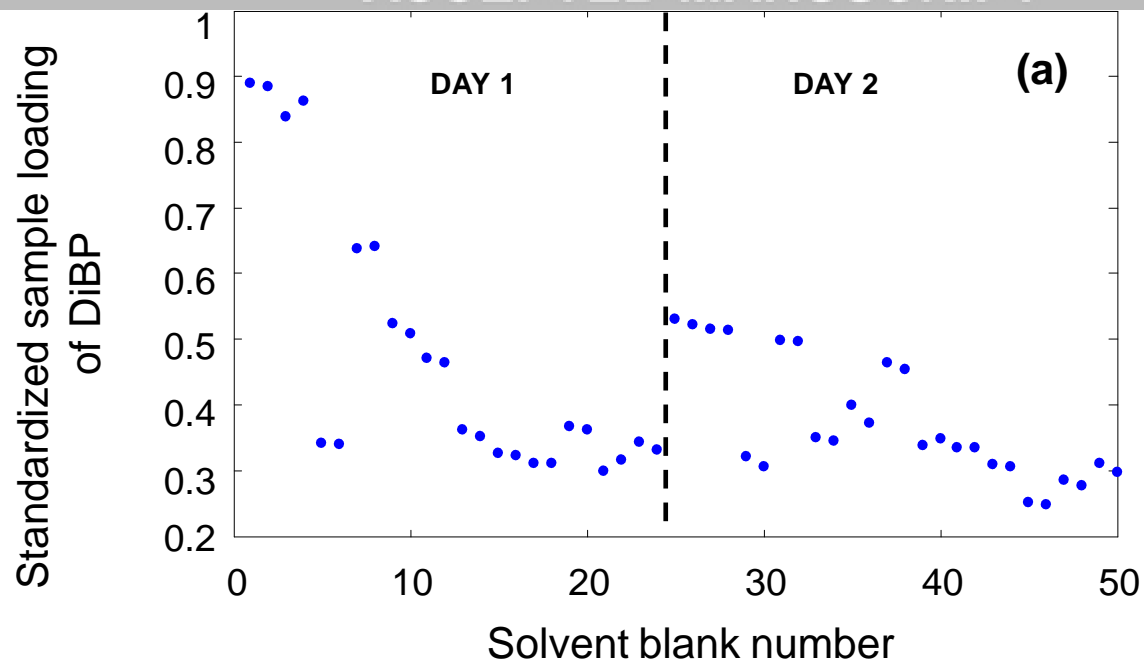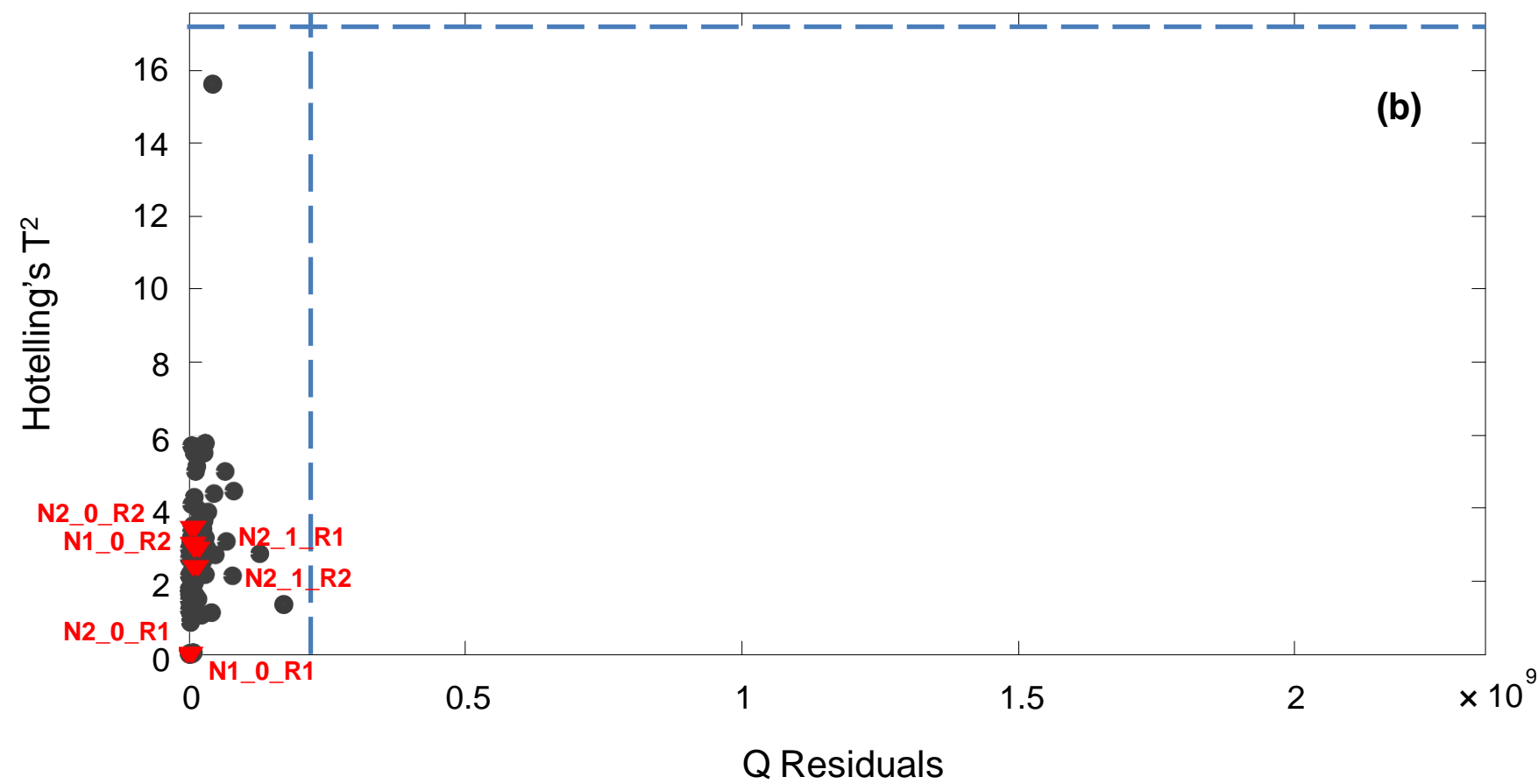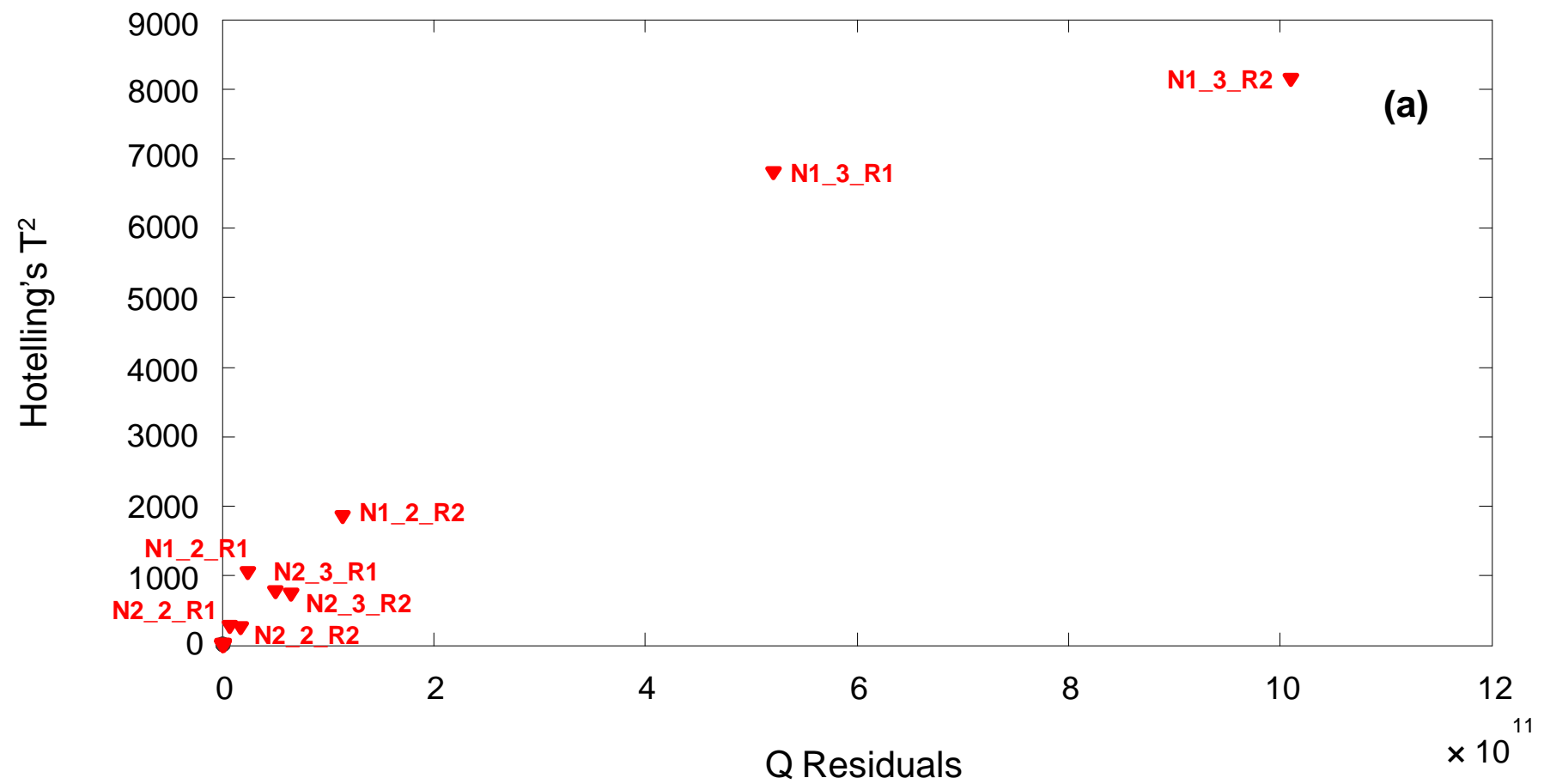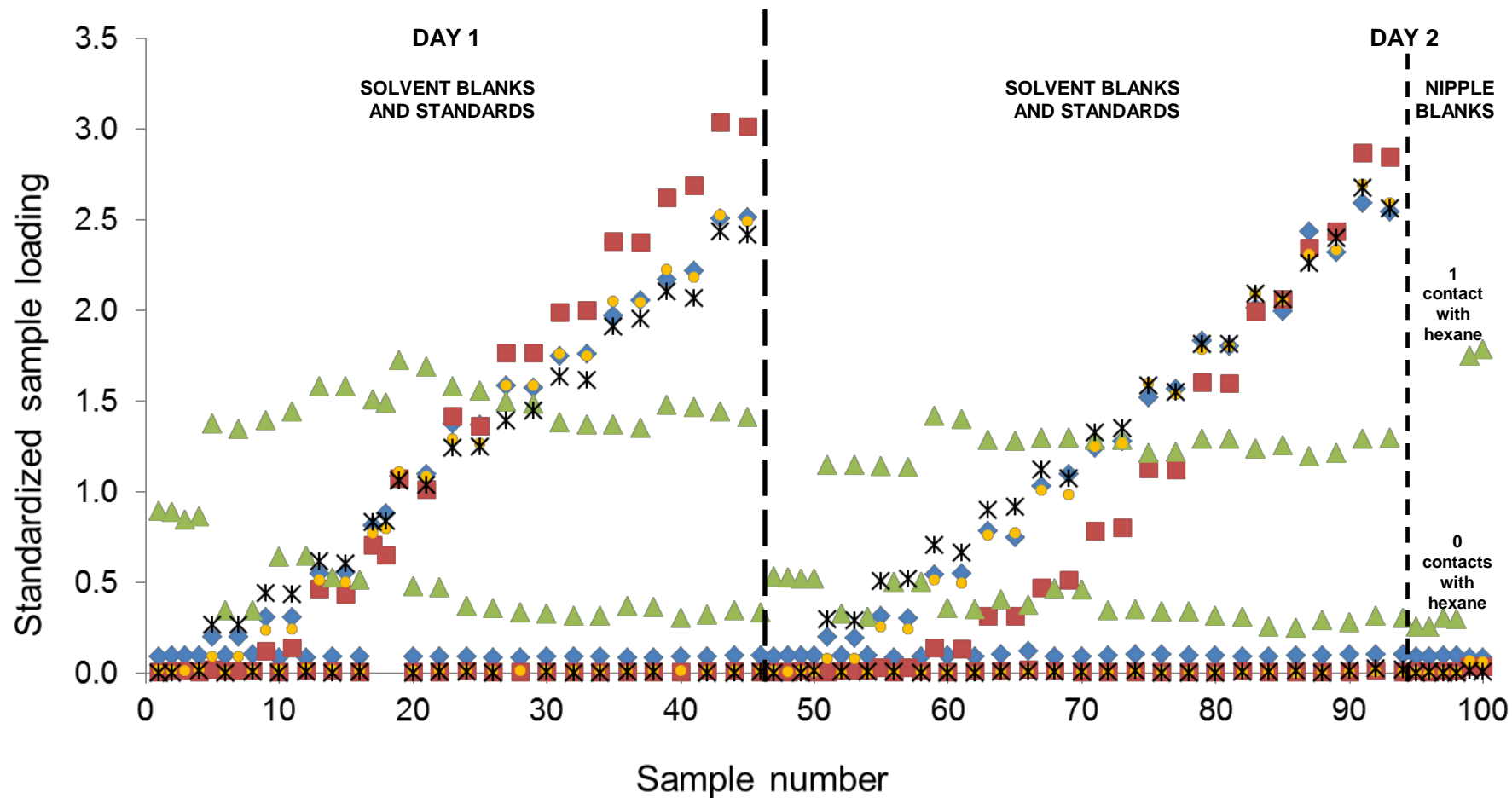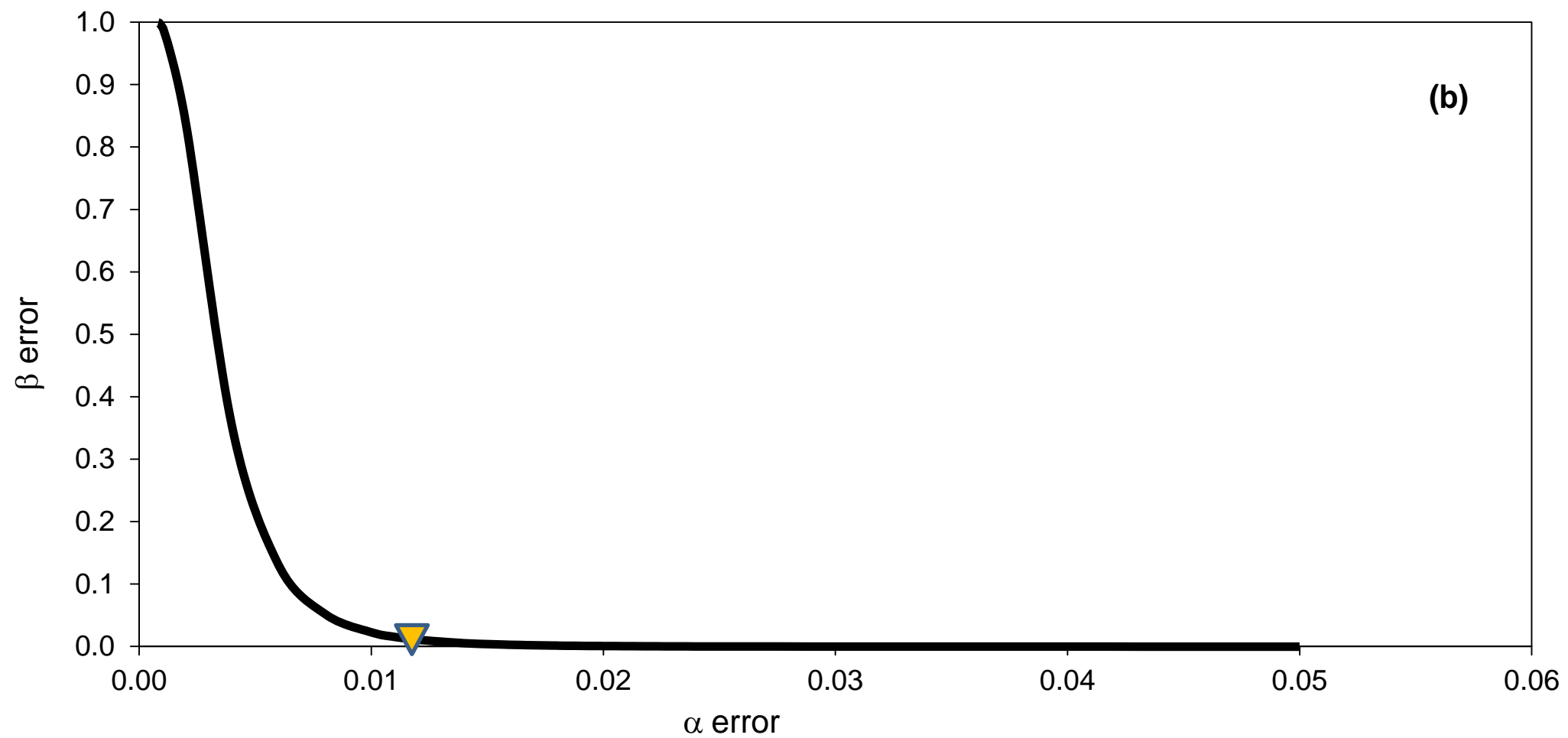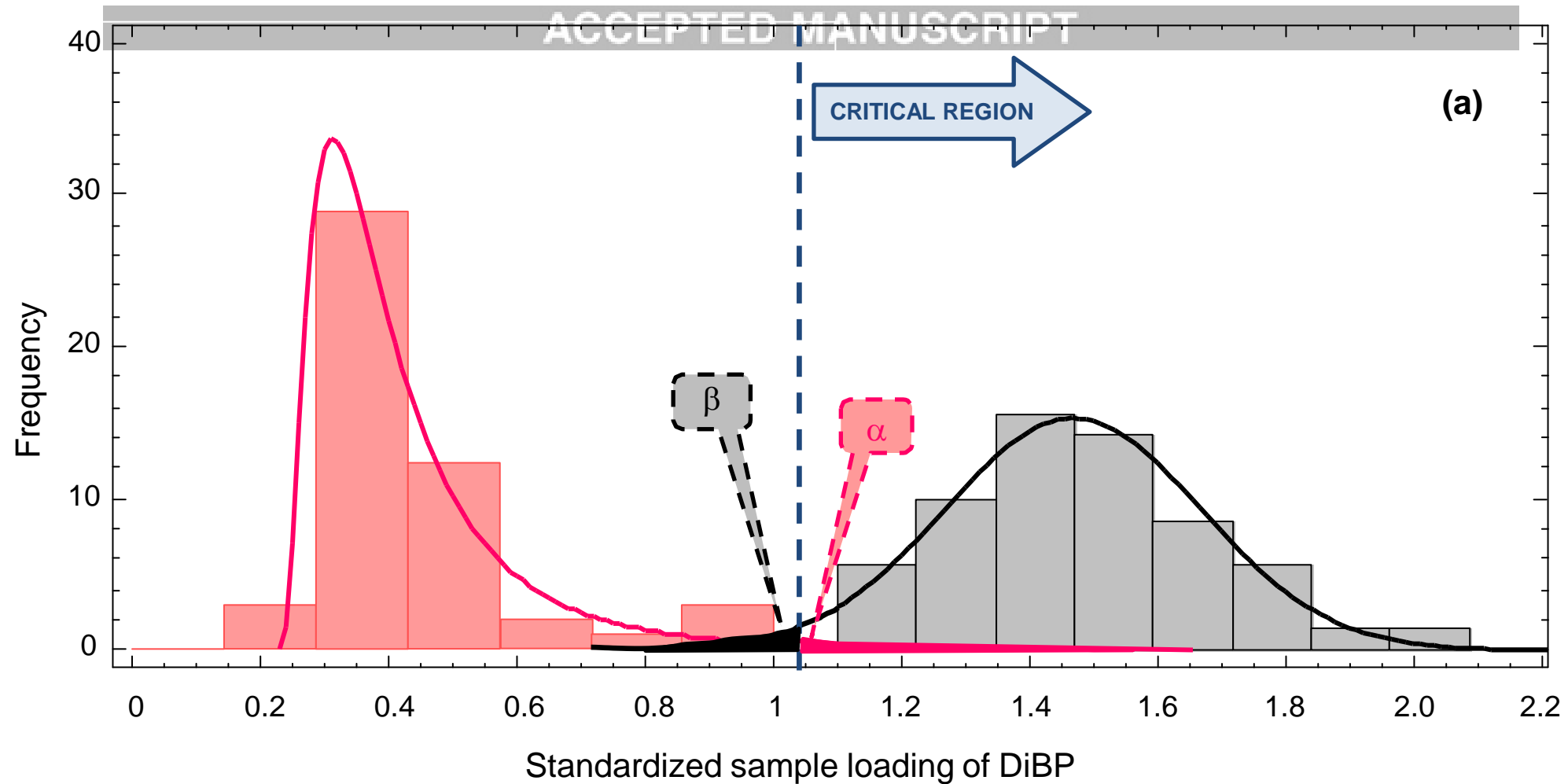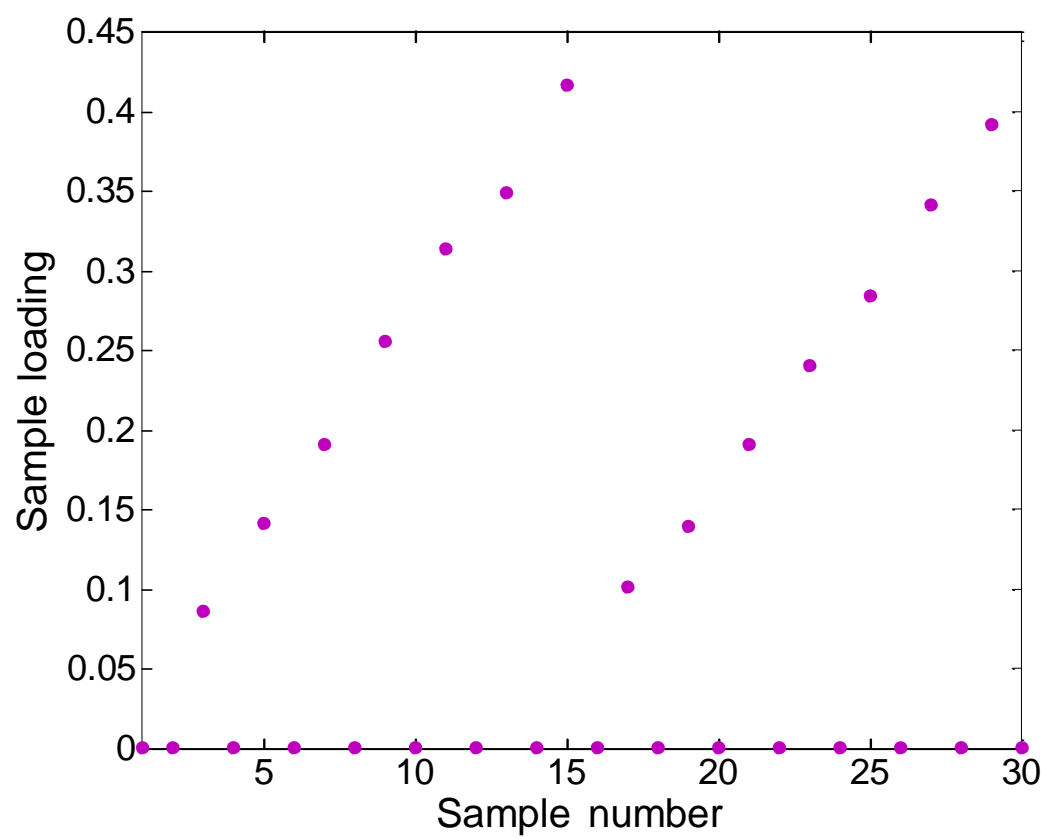
Fig. 8

Table 1 Summary of the samples analysed, concentration ranges and dimensions of the data tensors built for the analytes in each experimental stage of this work

Experimental stage	Samples analysed	Concentration range	Dimension of the resulting data tensor (scans × ions × samples)				
			BHT	BP	DiBP and DiBP-d_4	DEHA	DiNP
Tolerance intervals	3 system blanks 1 solvent blank without IS 6 reference standards	10-50 µg L^{-1} (for BHT, BP, DiBP and DiBP-d_4) 25-75 µg L^{-1} (for DEHA) 1-3 mg L^{-1} (for DiNP)	21 × 5 × 10	32 × 5 × 10	41 × 10 × 10	19 × 5 × 10	823 × 6 × 10
Calibration	8 system blanks[a] 1 solvent blank without IS[a] 22 solvent blanks with IS[a] 22 standards at 11 non- zero concentration levels (in duplicate) + 2 solvent blanks	0-50 µg L^{-1} (for BHT, BP) 25 µg L^{-1} of DiBP and DiBP-d_4 0-80 µg L^{-1} (for DEHA) 0-3 mg L^{-1} (for DiNP)	21 × 5 × 55	32 × 5 × 55	41 × 10 × 55	19 × 5 × 55	823 × 6 × 55
Procedure to assess the level of DiBP	18 system blanks 2 solvent blanks without IS 50 (24, 1st day + 26, 2nd day) solvent blanks with IS 44 (22, 1st day + 22, 2nd day) standards at 11 concentration levels (in quadruplicate) 16 extracts after contact with latex rubber nipples	0-50 µg L^{-1} (for BHT, BP) 25 µg L^{-1} of DiBP and DiBP-d_4 0-80 µg L^{-1} (for DEHA) 0-3 mg L^{-1} (for DiNP)	21 × 5 × 130	32 × 5 × 130	41 × 10 × 119 (11 outlier samples rejected)	19 × 5 × 130	823 × 6 × 130
Study of the matrix effect	8 system blanks 1 solvent blank without IS 6 solvent blanks and 6 solvent standards measured before matrix-matched standards 12 matrix-matched standards 6 solvent blanks and 6 solvent standards measured after matrix-matched standards	0-45 µg L^{-1} (for BHT, BP) 0-75 µg L^{-1} (for DiBP) 25 µg L^{-1} of DiBP-d_4 0-56 µg L^{-1} (for DEHA) 0-2.5 mg L^{-1} (for DiNP)	21 × 5 × 45	32 × 5 × 45	41 × 10 × 45	36 × 5 × 45	823 × 6 × 45

| Extraction from a dummy | 15 system blanks
1 solvent blank without IS
14 matrix-matched standards at 7 concentration levels (in duplicate) | 0-450 µg L^{-1} (for BHT)
0-12 µg L^{-1} (for BP)
0-40 µg L^{-1} (for DiBP)
0-48 µg L^{-1} (for DEHA)
0-1.5 mg L^{-1} (for DiNP)
DiBP-d$_4$: 25 µg L^{-1} and 225 µg L^{-1} (for the 1st and 2nd standard addition method, respectively) | 21 × 5 × 30 | 32 × 5 × 30 | 41 × 10 × 30 (in both analyses) | 19 × 5 × 30 | 823 × 6 × 30 |

[a] These samples have been considered in the PARAFAC decomposition but not in the estimation of the calibration model.

Table 2 Characteristics of the PARAFAC decomposition performed with the tensor built with the reference samples for each analyte (see Table 1, first row) and tolerance intervals for the relative retention time and the diagnostic ions in each case. The base peak is in bold

Analyte	PARAFAC model	Retention time			Diagnostic ions			
		t_R (min)	Relative t_R	Tolerance interval	m/z ratio	Spectral loading	Relative abundance (%)	Tolerance interval (%)
BHT	1 factor Unconstrained model Explained variance: 99.85%	8.401	0.808	(0.804-0.813)	91	6.85×10^{-2}	7.13	(3.57-10.70)
					145	1.14×10^{-1}	11.85	(9.48-14.22)
					177	7.95×10^{-2}	8.27	(4.14-12.41)
					205	9.61×10^{-1}	100.00	-
					220	2.28×10^{-1}	23.73	(20.17-27.29)
BP	1 factor Unconstrained model Explained variance: 92.72%	9.177	0.883	(0.879-0.888)	51	1.62×10^{-1}	21.03	(17.88-24.18)
					77	4.74×10^{-1}	61.70	(55.53-67.87)
					105	7.68×10^{-1}	100.00	-
					152	3.05×10^{-2}	3.97	(1.99-5.96)
					182	3.97×10^{-1}	51.68	(46.51-56.85)
DiBP-d$_4$	3 factors (Factor 2: DiBP-d$_4$) Non-negativity constraint in modes 1 and 2 Explained variance: 99.36% CORCONDIA: 98%	10.391	1.000	-	80	6.49×10^{-2}	6.52	(3.26-9.78)
					153	9.96×10^{-1}	100.00	-
					171	2.43×10^{-2}	2.44	(1.22-3.66)
					209	1.67×10^{-2}	1.68	(0.84-2.52)
					227	5.25×10^{-2}	5.27	(2.64-7.91)
DiBP	3 factors (Factor 1: DiBP) Non-negativity constraint in modes 1 and 2 Explained variance: 99.36% CORCONDIA: 98%	10.397	1.001	(0.996-1.006)	104	7.86×10^{-2}	7.90	(3.95-11.85)
					149	9.95×10^{-1}	100.00	-
					167	2.85×10^{-2}	2.86	(1.43-4.29)
					205	1.41×10^{-2}	1.42	(0.71-2.13)
					223	5.50×10^{-2}	5.53	(2.77-8.30)
DEHA	1 factor Unconstrained model Explained variance: 98.47%	13.319	1.282	(1.275-1.288)	112	3.57×10^{-1}	38.82	(33.00-44.64)
					129	9.21×10^{-1}	100.00	-
					147	1.51×10^{-1}	16.36	(13.09-19.63)
					241	4.11×10^{-2}	4.46	(2.23-6.69)
					259	1.78×10^{-2}	1.93	(0.97-2.90)
DiNP	3 factors (Factor 1: DiNP) Non-negativity constraint in the three modes Explained variance: 99.62% CORCONDIA: 95%	---[a]	---[a]	---[a]	57	3.64×10^{-1}	39.71	(33.75-45.67)
					127	9.54×10^{-2}	10.42	(8.34-12.50)
					149	9.16×10^{-1}	100.00	-
					167	8.48×10^{-2}	9.26	(4.63-13.89)
					275	5.70×10^{-3}	0.62	(0.31-0.93)
					293	1.15×10^{-1}	12.61	(10.09-15.13)

[a] It is not possible to establish a retention time for DiNP.

Table 3 Characteristics of the PARAFAC models obtained in the calibration step, identification of every analyte according to the regulation and parameters of the calibration line "standardized loadings *vs* true concentration" and of the accuracy line. Decision limit (CCα) and capability of detection (CCβ) at $x_0 = 0$ (α = β = 0.05). The third column shows the relative retention time and the relative abundances (in brackets) estimated from the spectral loadings for each diagnostic ion. In bold, the non-compliant m/z ratio.

Analyte	PARAFAC model	Identification	Calibration line Model (R^2, s_{yx})	Error (%)[b]	Accuracy line Model (R^2, s_{yx})	CCα (x = 0) (µg L⁻¹)	CCβ[c] (x = 0) (µg L⁻¹)
BHT	1 factor Unconstrained model Explained variance: 99.70%	$t_{R,rel} = 0.808$ 91 (7.12%) 145 (11.79%) 177 (8.31%) 205 (100%) 220 (23.82%)	$y = 9.59 \cdot 10^{-2} + 4.68 \cdot 10^{-2}\,x$ (99.75%, 0.04)	5.37% (n = 22)	$y = -8.89 \cdot 10^{-5} + 1.00\,x$ (99.75%, 0.86)	1.16	2.30
BP	1 factor Unconstrained model Explained variance: 96.96%	$t_{R,rel} = 0.884$ 51 (19.60%) 77 (59.12%) 105 (100%) 152 (4.21%) 182 (55.54%)	$y = -7.27 \cdot 10^{-2} + 4 \cdot 10^{-2}\,x + 2.98 \cdot 10^{-4}\,x^2$ (99.74%, 0.049)	5.72% (n = 22)	$y = 4.82 \cdot 10^{-3} + 1.00\,x$ (99.67%, 0.99)	1.34	2.66
DiBP-d₄	3 factors (Factor 2: DiBP-d₄) Non-negativity constraint in modes 1 and 2 Explained variance: 99.39% CORCONDIA: 98%	$t_{R,rel} = 1.000$ 80 (6.12%) 153 (100%) 171 (2.62%) 209 (1.57%) 227 (5.16%)	Internal standard		Internal standard		
DiBP	3 factors (Factor 1: DiBP) Non-negativity constraint in modes 1 and 2 Explained variance: 99.39% CORCONDIA: 98%	$t_{R,rel} = 1.001$ 104 (7.83%) 149 (100%) 167 (2.84%) 205 (1.47%) 223 (5.33%)	Not quantified		Not quantified		
DEHA	1 factor Unconstrained model Explained variance: 99.45%	$t_{R,rel} = 1.282$ 112 (35.92%) 129 (100%) 147 (16.04%) 241 (4.48%) 259 (1.89%)	$y = 1.12 \cdot 10^{-2} + 3.09 \cdot 10^{-2}\,x$ (99.75%, 0.04)	6.71% (n = 22)	$y = -7.54 \cdot 10^{-4} + 1.00\,x$ (99.75%, 1.36)	1.84	3.65

| DiNP | 2 factors (Factor 1: DiNP) Non-negativity constraint in modes 1 and 2 Explained variance: 99.75% CORCONDIA: 100% | $t_{R,rel}$ = -[a] **57** (32.52%) 127 (10.34%) 149 (100%) 167 (9.48%) 275 (0.63%) 293 (12.98%) | $y = -1.96 \cdot 10^{-2} + 5.81 \cdot 10^{-4}\,x + 8.15 \cdot 10^{-8}\,x^2$ (99.83%, $3.34 \cdot 10^{-2}$) | 2.33% (n = 22) | $y = 3.91 \cdot 10^{-2} + 1.00\,x$ (99.85%, 36.46) | 51.42 | 101.70 |

[a] It is not possible to establish a retention time for DiNP.

[b] Mean of the absolute value of the relative error in calibration.

[c] The first standard analysed was at a concentration of 2.5 µg L^{-1} for BHT, 4 µg L^{-1} for DEHA and 500 µg L^{-1} for DiNP which corresponds to a β value of 0.028, 0.025 and lower than 10^{-15}, respectively

Table 4 Comparison between solvent and matrix-matched calibrations to evaluate matrix effects

Analyte	PARAFAC/PARAFAC2 model (Outliers)	Solvent calibration (before matrix-matched analysis – C1 set –)		Matrix-matched calibration (C2 set)		Solvent calibration (after matrix-matched analysis – C3 set –)		p-values[c]
		$SSL^a = f(c_{true})$ $(R^2; s_{yx})$ (Outliers)	$c_{pred} = b_0 + b_1 \cdot c_{true}$ $(R^2; s_{yx})$	$SSL = f(c_{true})$ $(R^2; s_{yx})$ (Outliers)	$c_{pred} = b_0 + b_1 \cdot c_{true}$ $(R^2; s_{yx})$	$SSL = f(c_{true})$ $(R^2; s_{yx})$ (Outliers)	$c_{pred} = b_0 + b_1 \cdot c_{true}$ $(R^2; s_{yx})$	
BHT	1 factor (PARAFAC) Unconstrained model EV^b: 99.11% (0/45)	$y = 1.0\ 10^{-1} + 5.1\ 10^{-2}x$ (99.65%; 0.06) (0/12)	$y = -8.3\ 10^{-4} + 1.0x$ (99.65%; 1.12)	$y = 1.3\ 10^{-1} + 2.9\ 10^{-2}x$ (99.73%; 0.03) (1/12)	$y = -7.0\ 10^{-4} + 1.0x$ (99.73%; 0.88)	$y = 1.0\ 10^{-1} + 4.9\ 10^{-2}x$ (99.96%; 0.02) (1/12)	$y = 0.0 + 1.0x$ (99.96%; 0.34)	p-value $(\alpha_0) = 0.32$ p-value $(\alpha_1) = 0.00$ p-value $(\alpha_2) = 0.83$ p-value $(\alpha_3) = 0.01$
BP	1 factor (PARAFAC) Unconstrained model EV: 89.89% (0/45)	$y = 1.7\ 10^{-3} - 8.2\ 10^{-4}x + 8.9\ 10^{-4}x^2$ (99.56%; 0.05) (0/12)	$y = 1.44 + 0.96x$ (99.44%; 1.37)	$y = 7.7\ 10^{-2} + 4.0\ 10^{-2}x$ (99.97%; 0.01) (0/12)	$y = 7.8\ 10^{-4} + 1.0x$ (99.97%; 0.31)	$y = -2.5\ 10^{-3} + 1.8\ 10^{-2}x + 5.7\ 10^{-4}x^2$ (99.67%; 0.05) (0/12)	$y = 8.7\ 10^{-2} + 1.0x$ (99.73%; 0.98)	_____
DiBP	2 factors (PARAFAC2) Non-negativity constraint in mode 2 EV: 99.99% CORCONDIA: 100% (0/45)	$y = 1.7\ 10^{-2} + 4.2\ 10^{-3}x$ (99.99%; 0.001) (1/12)	$y = 1.5\ 10^{-3} + 1.0x$ (99.99%; 0.31)	$y = 1.14 + 3.2\ 10^{-3}x + 2.2\ 10^{-5}x^2$ (98.96%; 0.02) (0/12)	$y = -1.8\ 10^{-2} + 1.0x$ (98.68%; 3.66)	$y = 1.7\ 10^{-2} + 4.3\ 10^{-3}x$ (99.87%; 0.005) (1/12)	$y = 2.3\ 10^{-3} + 1.0x$ (99.87%; 1.13)	_____
DEHA	2 factors (PARAFAC) Non-negativity constraint in mode 1 EV: 99.50% CORCONDIA: 100% (0/45)	$y = 1.3\ 10^{-1} + 2.2\ 10^{-2}x$ (99.25%; 0.05) (0/12)	$y = 2.3\ 10^{-2} + 1.0x$ (99.25%; 2.09)	$y = 6.5\ 10^{-1} + 1.8\ 10^{-2}x$ (98.04%; 0.06) (0/12)	$y = -9.7\ 10^{-3} + 1.0x$ (98.04%; 3.42)	$y = 9.5\ 10^{-2} + 1.9\ 10^{-2}x$ (99.84%; 0.02) (0/12)	$y = -6.8\ 10^{-4} + 1.0x$ (99.83%; 0.99)	p-value $(\alpha_0) = 0.22$ p-value $(\alpha_1) = 0.00$ p-value $(\alpha_2) = 0.00$ p-value $(\alpha_3) = 0.00$

| DiNP | 3 factors (PARAFAC) Non-negativity constraint in all modes EV: 96.05% CORCONDIA: 89% (0/45) | $y = 1.7\ 10^{-2}$ $+ 8.9\ 10^{-4}x$ (99.65%; 0.06) (0/12) | $y = -3.0\ 10^{-2} + 1.0x$ (99.65%; 63.55) | $y = -1.5\ 10^{-2}$ $+ 6.6\ 10^{-4}x$ (99.25%; 0.06) (0/12) | $y = -5.7\ 10^{-2} + 1.0x$ (99.25%; 92.83) | $y = 4.0\ 10^{-3}$ $+ 8.0\ 10^{-4}x$ (99.46%; 0.06) (0/12) | $y = 3.0\ 10^{-2} + 1.0x$ (99.46%; 79.11) | p-value (α_0) = 0.70 p-value (α_1) = 0.00 p-value (α_2) = 0.34 p-value (α_3) = 0.00 |

[a] Standardized sample loading

[b] Explained variance

[c] p-values for the hypothesis test on the significance of the estimates of the α-coefficients in Eq. (3)

Table 5 PARAFAC models estimated with the data from the extraction study, identification of every analyte according to the regulation and results obtained with the standard addition method. The third column shows the relative retention time and the relative abundances (in brackets) estimated from the PARAFAC spectral loadings for each diagnostic ion. In bold, the non-compliant m/z ratios.

Analyte	PARAFAC model	Identification	LS regression "standardized sample loadings *versus* added concentration"		Accuracy line	Sample concentration ($\mu g\ L^{-1}$)	Interval (at 95% confidence level)	Conclusions
			Model (R^2, s_{yx})	Error (%) [c]	Model (R^2, s_{yx})			
BHT	1 factor Unconstrained model Explained variance: 99.88%	$t_{R,rel}$ = 0.808 91 (5.98%) 145 (10.99%) 177 (7.55%) 205 (100%) 220 (24.06%)	y = $3.84 \cdot 10^{-1}$ + $2.34 \cdot 10^{-3}$ x (n = 12) (99.24%, $2.87 \cdot 10^{-2}$)	4.50% (n = 10)	y = $1.44 \cdot 10^{-1}$ + 1.00 x (99.24%, 12.25)	37.87	(31.23, 45.13)	BHT detected
BP	1 factor Unconstrained model Explained variance: 99.33%	$t_{R,rel}$ = 0.882 51 (18.83%) 77 (58.15%) 105 (100%) 152 (3.80%) **182** (57.68%)	y = $6.72 \cdot 10^{-1}$ + $4.89 \cdot 10^{-2}$ x (n = 14) (96.94%, $3.76 \cdot 10^{-2}$)	10.77% (n = 12)	y = $5.18 \cdot 10^{-3}$ + 1.00 x (96.93%, $7.69 \cdot 10^{-1}$)	0.92	(0.76, 1.1)	Below its CCα
DiBP-d₄	1st standard addition method: 3 factors [a] (Factor 2: DiBP-d₄) Non-negativity constraint in mode 2 Explained variance: 99.99% CORCONDIA: 99.72%	$t_{R,rel}$ = 1.000 80 (5.72%) 153 (100%) 171 (2.11%) 209 (1.47%) 227 (5.45%)	Internal standard		Internal standard		Internal standard	
	2nd standard addition method: 2 factors (Factor 1: DiBP-d₄) Non-negativity constraint in modes 1 and 2 Explained variance: 99.71% CORCONDIA: 100%	$t_{R,rel}$ = 1.000 min 80 (5.25%) 153 (100%) 171 (2.70%) 209 (1.40%) 227 (5.69%)	Internal standard		Internal standard		Internal standard	
DiBP	1st standard addition method: 3 factors [a] (Factor 3: DiBP) Non-negativity constraint in mode 2 Explained variance: 99.99%	$t_{R,rel}$ = 1.001 104 (6.82%) 149 (100%) 167 (3.23%) 205 (1.65%)	y = $4.00 \cdot 10^{-1}$ + $2.03 \cdot 10^{-2}$ x (n = 10) (99.01%, $2.77 \cdot 10^{-2}$)	3.15% (n = 8)	y = $-7.39 \cdot 10^{-4}$ + 1.00 x (99.01%, 1.36)	1.31	(1.04, 1.62)	Below the level fixed at 25 $\mu g\ L^{-1}$

		CORCONDIA: 99.72%	223 (6.47%)						
DEHA	3 factors (Factor 1: DEHA) Non-negativity constraint in modes 1 and 2 Explained variance: 99.33% CORCONDIA: 96%	$t_{R,rel}$ = 1.282 **112** (23.62%) 129 (100%) 147 (18.86%) 241 (5.41%) **259** (3.31%)	$y = 1.47 \cdot 10^{-2} + 3.26 \cdot 10^{-2} x$ (n = 14) (99.45%, $4.21 \cdot 10^{-2}$)	3.60% (n = 12)	$y = -1.07 \cdot 10^{-3} + 1.00 x$ (99.45%, 1.29)	0.03	(-0.13, 0.19)	The confidence interval contained zero
DiNP	3 factors [a] (Factor 2: DiNP) Non-negativity constraint in modes 2 and 3 Explained variance: 99.99% CORCONDIA: 94.95%	$t_{R,rel}$ = -[b] 57 (43.88%) 127 (8.80%) 149 (100%) 167 (9.16%) **275** (0.01%) **293** (15.75%)	$y = 5.86 \cdot 10^{-3} + 9.91 \cdot 10^{-4} x$ (n = 12) (95.89%, $9.59 \cdot 10^{-2}$)	12.93% (n = 10)	$y = -3.57 \cdot 10^{-3} + 1.00 x$ (95.89%, 96.80)	0.394	(-11.44, 14.06)	The confidence interval contained zero

[a] PARAFAC2 model.

[b] It is not possible to establish a retention time for DiNP.

[c] Mean of the absolute value of the relative error in calibration.